Publication No. U-3663
W. O. No. 2354-0000

Under Contract: NAS8-20503

22 June 1966

FINAL REPORT

INSTRUMENT DEVELOPMENT FOR THE BASE FLOW REGION OF A MULTINOZZLE BOOSTER VEHICLE

Prepared for: George C. Marshall Space Flight Center
National Aeronautics and Space Administration
Huntsville, Alabama

Period Covered: June 23, 1965 through June 22, 1966

Prepared by: A. B. Bauer

Approved by: P. M. Sutton
P. M. Sutton
Manager
Physics Laboratory

AERONUTRONIC
DIVISION OF PHILCO CORPORATION
A SUBSIDIARY OF Ford Motor Company
FORD ROAD · NEWPORT BEACH, CALIFORNIA

CONTENTS

SECTION		PAGE
1	INTRODUCTION	1
2	PROBE CONSTRUCTION AND OPERATION	3
3	PROBE TIP AND HOT-WIRE CONSTRUCTION.	17
4	VELOCITY MEASUREMENT TESTS IN SUBSONIC FLOW	
	4.1 Pulse Length and Amplitude.	23
	4.2 Second Wire Current and Signal Amplification. . .	24
	4.3 Oscilloscope Screen Display	24
	4.4 Effect of Wire No. 1 Wake on t_o	27
	4.5 Velocity Measurements	31
5	VELOCITY MEASUREMENT TESTS IN SUPERSONIC FLOW.	34
6	PROBE DATA REDUCTION METHOD	
	6.1 Hot-Wire Mean Temperature	37
	6.2 Data Reduction Procedure.	41
	6.3 Determination of Hot-Wire Calibration Constants .	48
	6.4 Use of Pitot and Static Tubes in Flow Field Measurements.	49
7	EXAMPLE OF THE FLOW FIELD MEASUREMENT BEHIND A CONE. .	51
	7.1 Velocity Vector Direction Measurements.	52
	7.2 Stream Variable Measurements and Data Reduction .	52

CONTENTS (Continued)

SECTION		PAGE
8	FLOW REGIME OF PROBE OPERATION	
	8.1 Limits of Probe Operation to Date	60
	8.2 Improvement in Probe Operating Limits Through Future Research	62
9	CONCLUSIONS.	64
10	REFERENCES	66

ILLUSTRATIONS

FIGURE		PAGE
1	Probe No. 3	4
2	Probe No. 3	5
3	Schematic Diagram of Probe Tips, Supporting Tubes, Front Hinge, and Linkage.	6
4	x, and y_1 Versus Revolutions of Screws No. 1 and 2 for Probes Two and Three.	8
5	x and y_1 Versus Revolutions of Screws No. 1 and 2 for Probe One	9
6	Wiring Diagram of Probe Three	12
7	External Control and Readout Circuit for Probe Three. .	13
8	Probe Tip and Hot Wire Element.	18
9	Examples of Probe Tip Configurations.	19
10	Schematic Diagram Showing the Essential Features of the Hot-Wire Voltages as Displayed on the Oscilloscope Screen.	25
11	A, Versus R_d and M.	30
12	Correlation of Velocity Defect Data for Subsonic Flow Subsonic Speeds	32

ILLUSTRATIONS (Continued)

FIGURE		PAGE
13	Measured Velocity Direction Vectors - Dots Show Point to which the Measurements Refer	53
14	Stream Parameters for X = 0.5 Diameter Behind the Cone.	54
15	Stream Parameters for X = 0.5 Diameter Behind the Cone.	55
16	Flow Regime Map Showing Range of Operation of the Two-Wire Probe to Date.	61

SECTION 1

INTRODUCTION

The purpose of the present investigation has been to develop a two-wire probe into an instrument capable of determining fluid velocity, pressure, density, and temperature in an unknown flow field. The idea, which has been described in References 1 and 2, makes use of two very small wire elements. When one wire is heated by a short pulse of electrical energy, it transfers heat to the flow. The heated flow is sensed by the second wire provided that the second wire is placed within the wake of the first wire. The time for the heated wake to travel between the wires may be used to determine the flow speed; the direction of the wake behind the first wire determines the velocity vector direction. The method of computing the flow speed also depends on two measurements of the hot-wire resistance at two different heating currents. The measurements are then used to compute the fluid pressure, density, and temperature.

The two wire elements are held in the airstream by four slender needles. The needles are, in turn, held in place by the probe structure. The probe is capable of positioning the two wires so that the wake of the first wire is intercepted by the second wire.

The probe mechanism and wire holders are described in Sections 2 and 3. Sections 4 and 5 describe probe tests in subsonic and supersonic streams. The method of converting the probe measurements into stream parameters is described in Section 6; a sample flow field measurement is given in Section 7. Section 8 describes the flow regime in which the probe may be operated; Section 8 suggests two areas of research that would be useful in extending the probe operating limits. Concluding statements are given in Section 9.

SECTION 2

PROBE CONSTRUCTION AND OPERATION

Three probe models have been designed and built. With one minor exception, the mechanics of the three probes are alike, and have been described earlier.[3] Figures 1 and 2 show photographs of the third probe to be built. The third probe is motor driven, whereas the first two probes are operable through three flexible shafts connected in place of the three motors of Figures 1 and 2.

Figure 3 shows the probe tips, the support tubes, and the front hinge. The dimensions x_2 and y_2 are defined on the figure for the condition that the linkage mechanism, which drives tube no. 1, be positioned at the right-angle configuration shown in the figure. This right-angle configuration also defines the zero or central position of the two screws which drive the linkage. One revolution of screw no. 1 drives wire no. 1 a nominal distance of $x_1 = 0.0100$ in, $y_1 = 0$. One revolution of screw no. 2 drives wire no. 1 a nominal distance of $x_1 = 0$ in, $y_1 = -0.0100$ in.

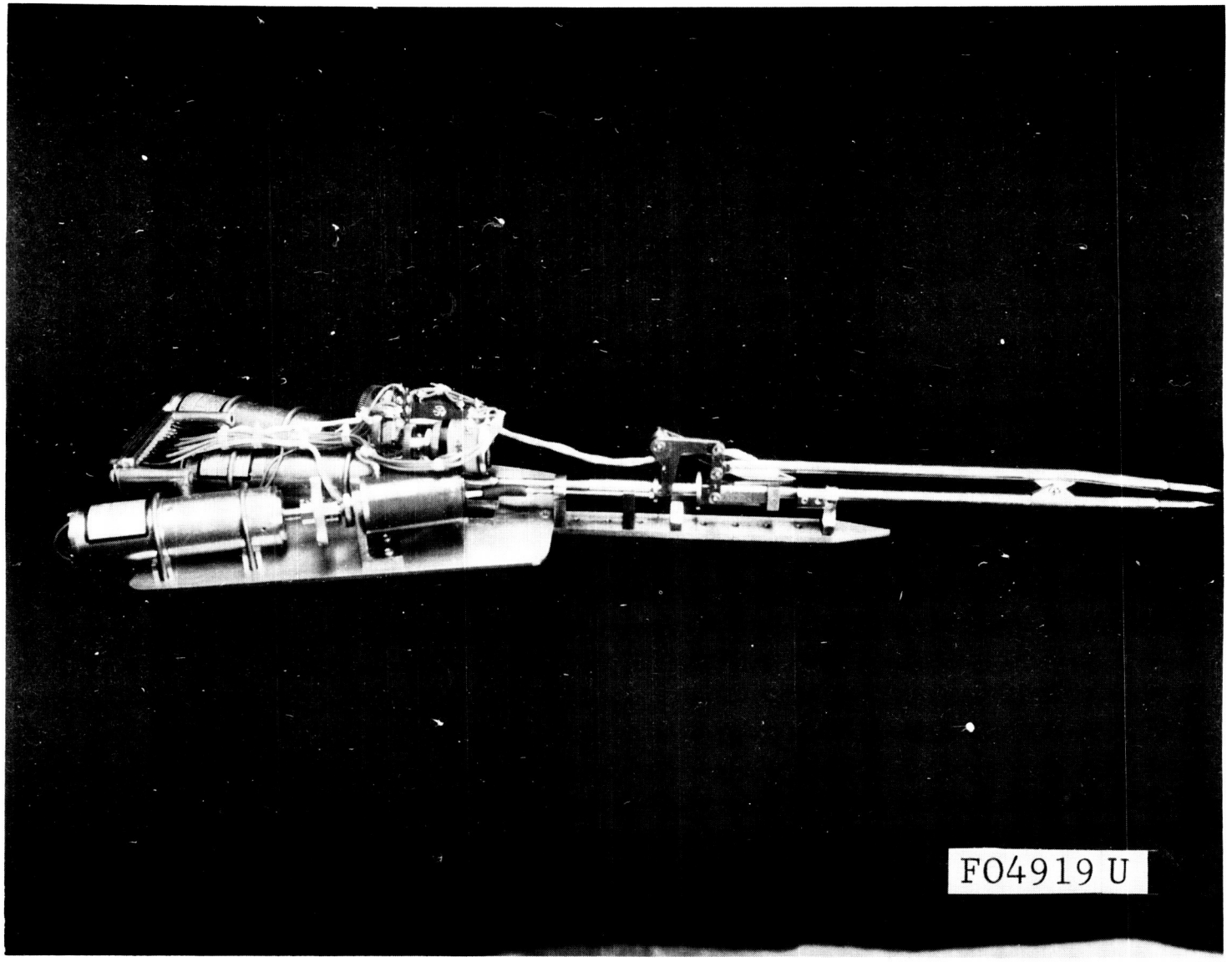

FIGURE 1. PROBE NO. 3

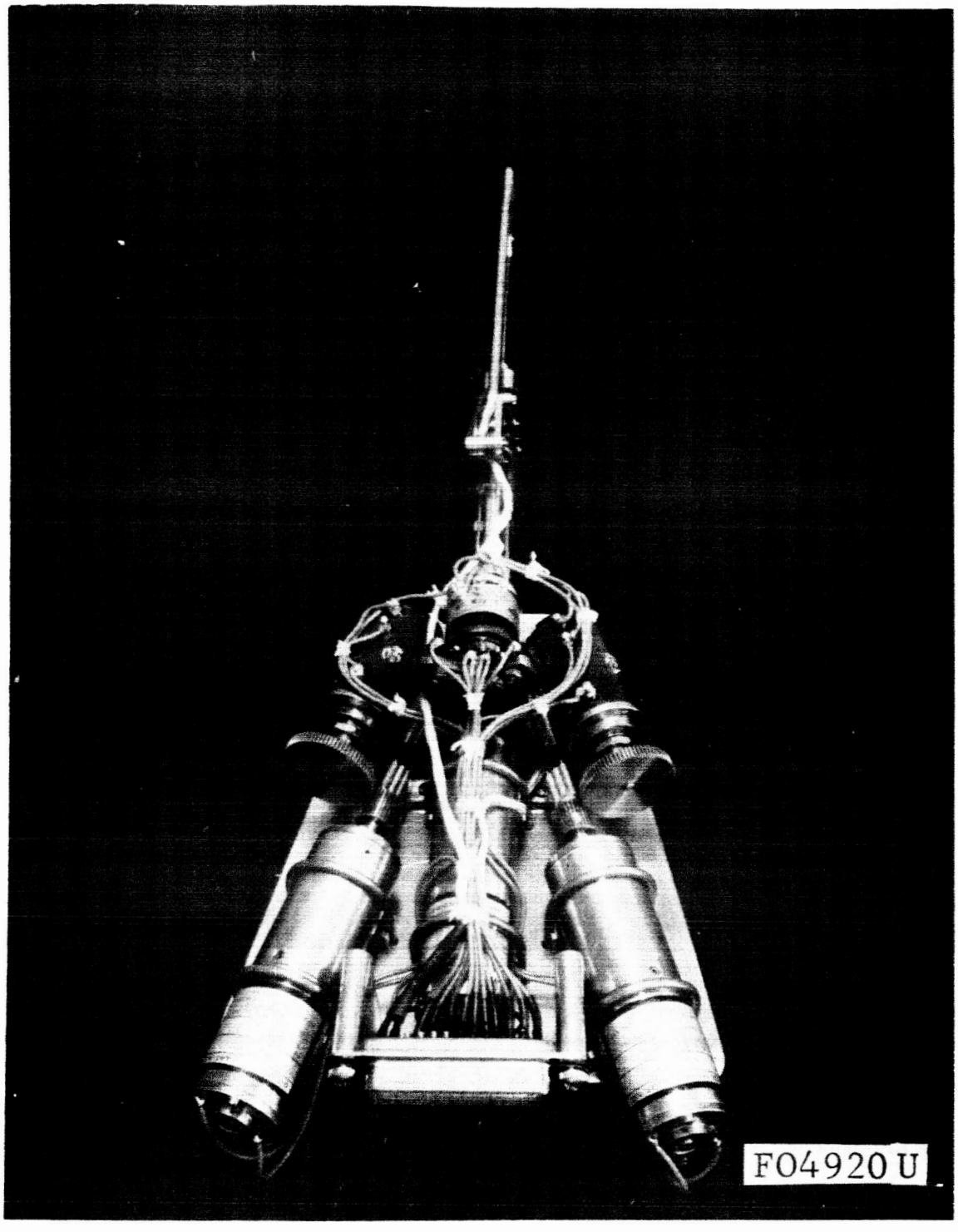

FIGURE 2. PROBE NO. 3

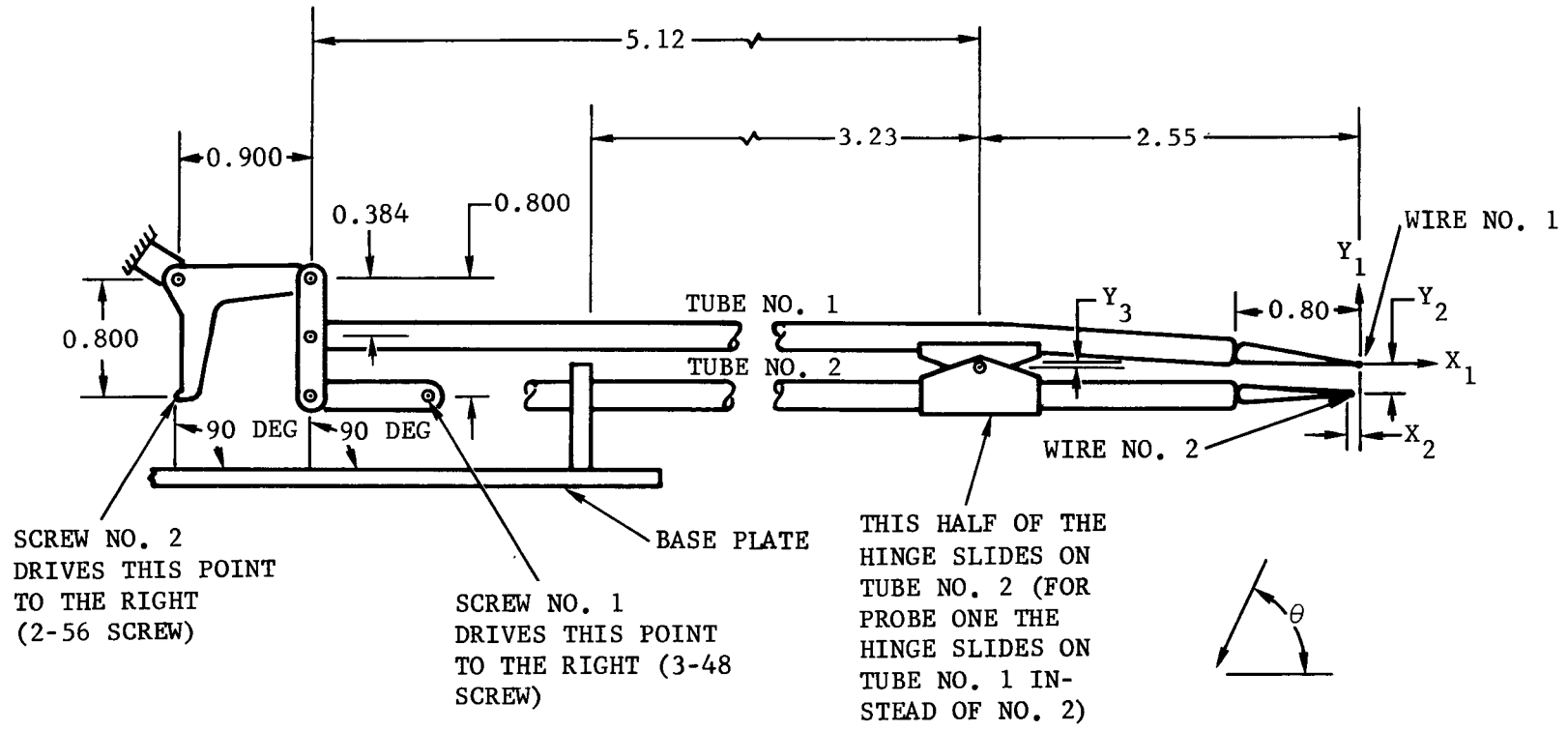

FO4921 U

FIGURE 3. SCHEMATIC DIAGRAM OF PROBE TIPS, SUPPORTING TUBES, FRONT HINGE, AND LINKAGE

The actual x_1 and y_1 motion is somewhat different from the nominal motion, and is given by Figure 4. (On probe one only, the front hinge is inverted so that it slides on tube 1 rather than on tube 2; also, for probe one, the 0.800 dimension on the probe tip is 1.100 in. Because of the hinge difference, use Figure 5 rather than Figure 4 for the x_1, y_1 motion on probe one.)

When the probe is operated so that wire 2 is at the center of the wake of wire 1, the flow angle θ measured with respect to the centerline of tube 2 is given by

$$\theta = \tan^{-1} \left(\frac{y_1 + y_2}{x_1 + x_2}\right) \qquad (2\text{-}1)$$

This angle is, of course, measured in the plane of tubes 1 and 2. This plane and the probe mechanism (linkage, both tubes and wires) rotate as a unit about the centerline of tube 2. The angle ϕ of this rotation and θ together determine uniquely the vector flow direction.

The angle ϕ should be determined in any flow field application before the angle θ is determined. This is done, as described in Reference 1, by rotating the probe about the ϕ axis until the voltage measured across wire 2 is a minimum, indicating that the stream is then normal to wire 2. Wire 1 could also be used for the same purpose provided that it is switched from the pulse generator to a constant current source. Maximum sensitivity of the wire voltage to angle ϕ occurs at the largest possible value of current; a suggested current value for wire 2 is 10 ma. In hunting for the proper ϕ, the operator should realize that if the stream

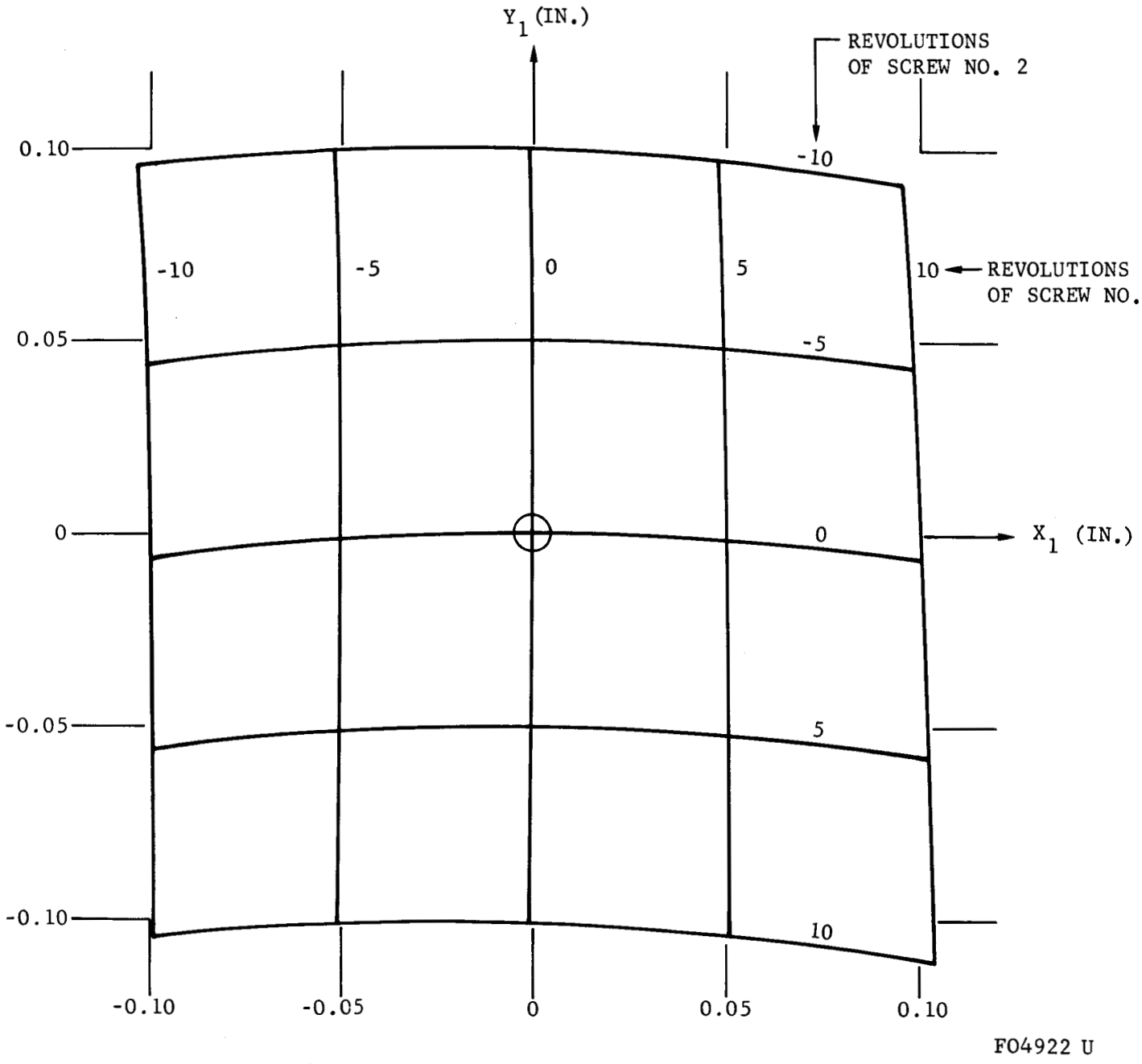

FIGURE 4. X_1 AND Y_1 VERSUS REVOLUTIONS OF SCREWS NO. 1 AND 2 FOR PROBES TWO AND THREE

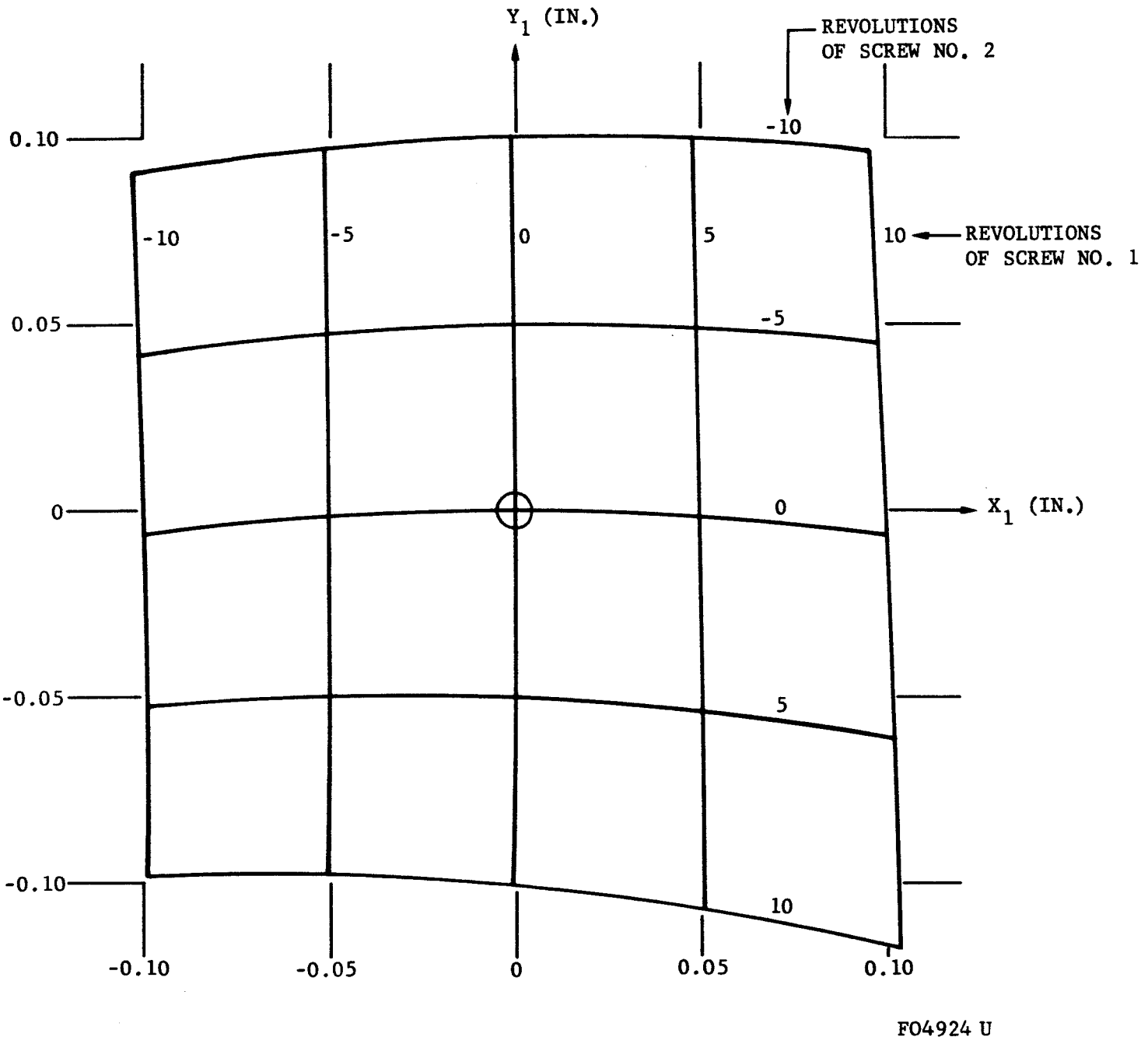

FIGURE 5. X_1 AND Y_1 VERSUS REVOLUTIONS OF SCREWS NO. 1 AND 2 FOR PROBE ONE

is parallel to the Ø axis (or nearly parallel), the wire will always be perpendicular (or nearly perpendicular) to the stream. Therefore, a lack of sensitivity of the voltage to angle Ø may be interpreted as a stream almost parallel to the Ø axis.

The 2.55 in dimension shown on Figure 3 is essential in order that the x_1, y_1 dimensions of Figures 4 and 5 be correct. On occasion, however, a probe tip of length different from the 0.800 in of Figure 3 may be utilized for wire 1. In this case a slight correction should be applied to the readings of Figures 4 and 5. If ℓ_1 is the new length of the 2.55 dimension, the new values of x_1 and y_1 are

$$x_{1_{new}} = x_1 \tag{2-2}$$

$$y_{1_{new}} = y_1 \left(\frac{\ell_1}{2.55}\right) \tag{2-3}$$

If the probe tip 1 is shaped considerably different from that of Figure 3, so that the wire is in a horizontal plane that is some distance y_3 above the front hinge line, an added correction is necessary to the value of x_1, so that

$$x_{1_{new}} = x_1 - \left(\frac{y_1}{\ell_1}\right) y_3 \tag{2-4}$$

This correction term is generally quite small.

A positive rotation of the two screws and/or the angle Ø is here defined as clockwise, as seen in the view of the probe given by Figure 2. Probes one and two are driven by flexible shafts equipped with "duodials" which record the shaft rotation on the face of the dial. For convenience,

the duodial faces should be positioned at zero when the probe linkage is in the right-angled configuration of Figure 3. Then the duodial reading represents the number of screw revolutions on Figures 4 and 5.

For probe three, electric motors drive the probe. As seen in Figure 2, the motor on the left, motor no. 1, drives screw no. 1. The motor on the right, motor no. 2, drives screw no. 2. The central motor, motor no. 3, drives the entire probe through the angle $\emptyset$. Each of the motors drive a position readout device or potentiometer through gears; the potentiometers are numbered 1, 2, and 3 corresponding to motors 1, 2, and 3.

All the electrical leads to the probe are brought out through a 25 pin Cannon plug, as shown at the bottom of Figure 2. The wiring of the probe and the required control circuit is shown on Figures 6 and 7. Terminals E and F must receive voltage of the indicated polarity; this enables the limit switches to function properly on motor 3. Switch 1 controls the direction of rotation of motor 3. The power supplies used on terminals AB and on CD run motors 1 and 2, respectively. A positive voltage on terminals A and C will run the motors so that x_1 and y_1, respectively, are increased. Terminals B and D are wired together and to the ground of the probe. For this reason, one power supply cannot be used simultaneously at AB and CD unless it is desired that both B and D have the same polarity. The speed of the drive motors is, of course, controlled by the applied voltage, which should not exceed 27 V. At 27 V, motors 1 and 2 will turn their output shafts at about 29 RPM; motor 3 will turn its output shaft at about 2.3 RPM.

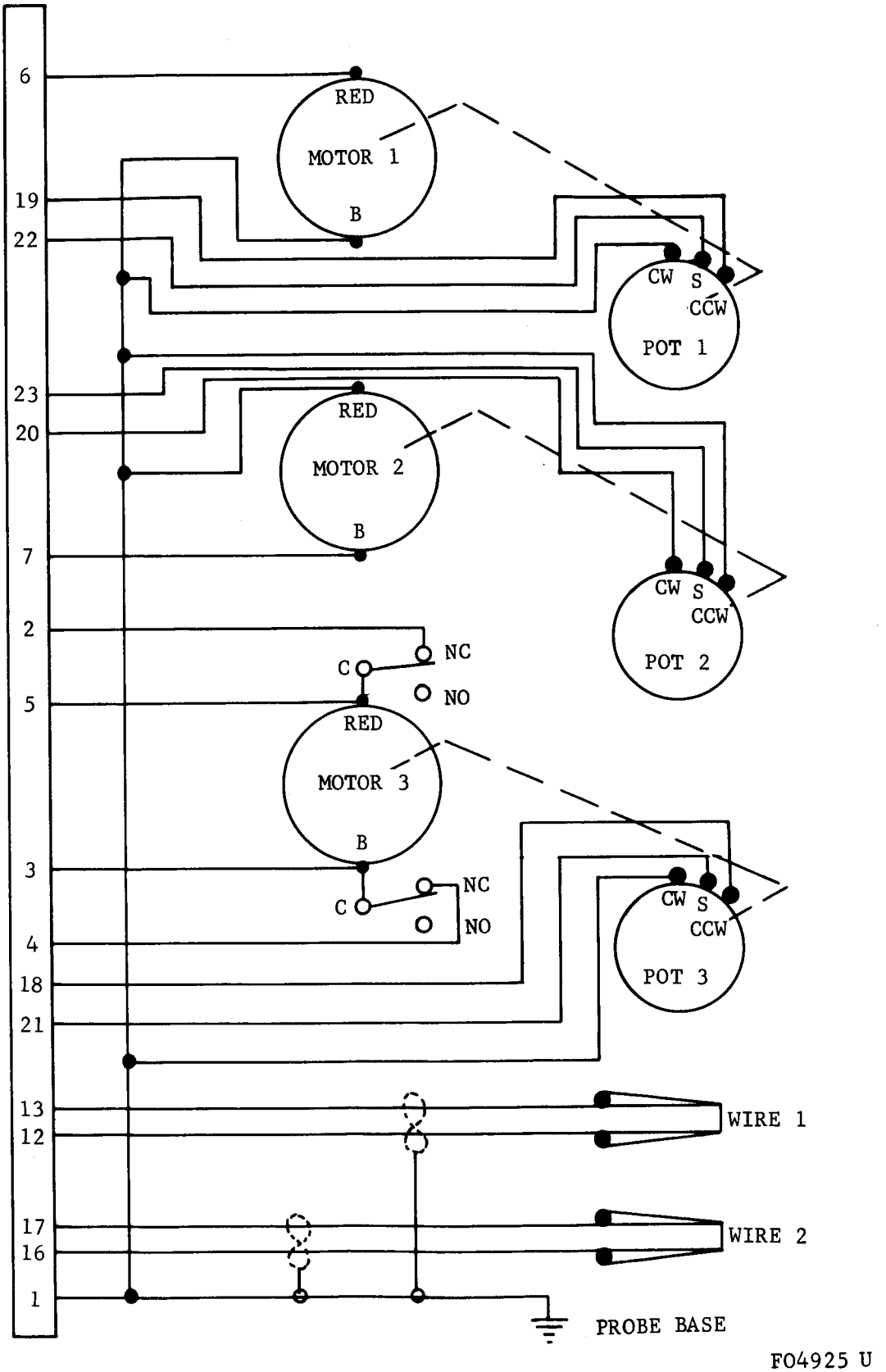

FIGURE 6. WIRING DIAGRAM OF PROBE 3

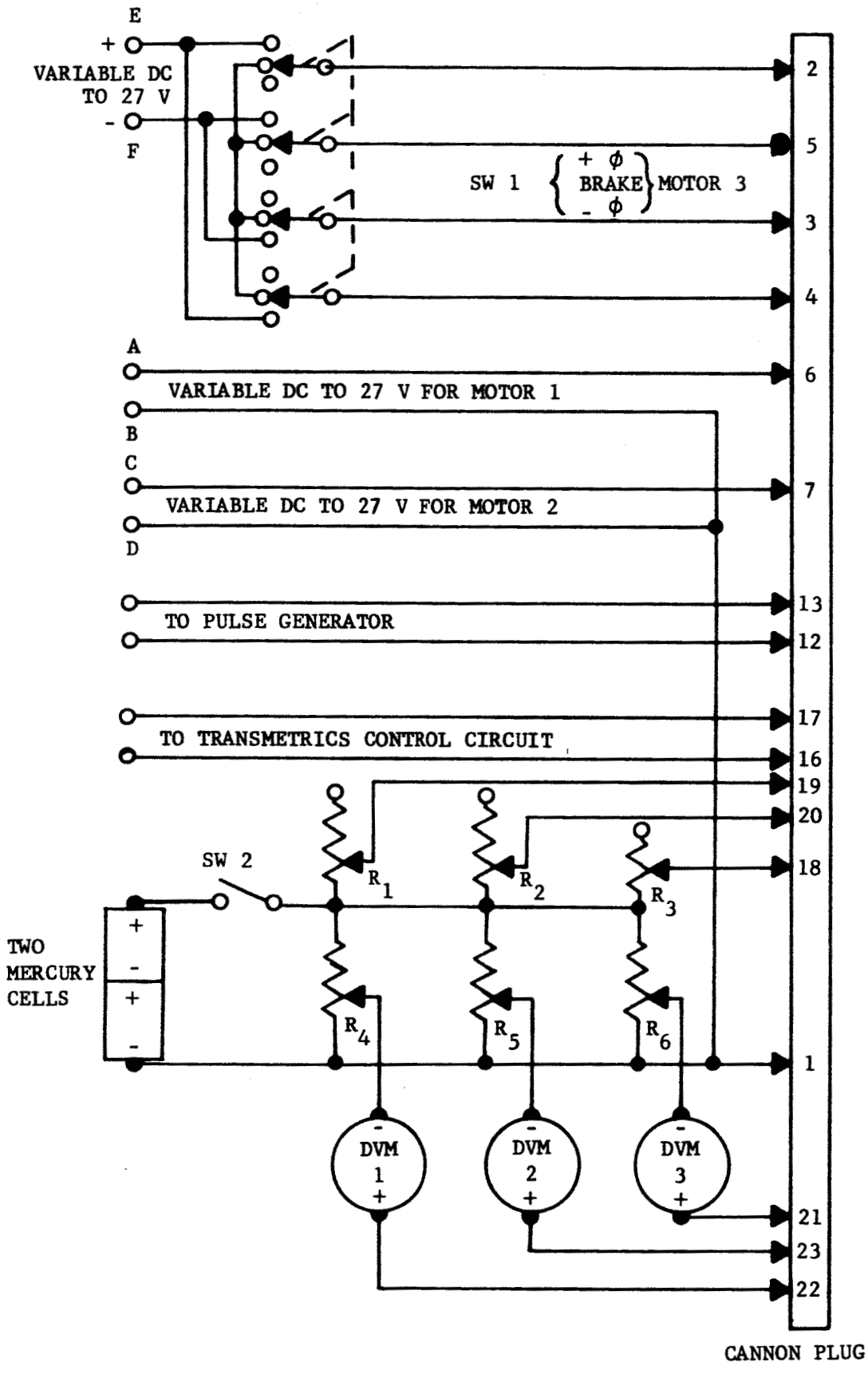

FO4926 U

FIGURE 7. EXTERNAL CONTROL AND READOUT CIRCUIT FOR PROBE 3

The required probe position readout circuit is shown on the lower part of Figure 7. (The circuits on Figure 7 are not supplied as a part of the present contract; therefore, Figure 7 represents only the suggested means of controlling and positioning the probe.) The circuit is powered by two mercury cells. The current drain on the cells is less than one ma; nevertheless it is suggested that cells about the size of an ordinary flashlight battery be used for long life without appreciable voltage variation. If desired, an inexpensive voltmeter can be added to monitor the total voltage output of the two cells, which will be about 2.70 volts for mercury cells in good condition. With this voltage, it is recommended that R_1 and R_2 be adjusted to about 800 ohms and R_3 to about 17,000 ohms. Then the output voltages read on the digital voltmeters will be near 0.100 V per revolution of screws 1 and 2, corresponding to a nominal movement of wire 1 of 0.010 in in both the x_1 and y_1 directions. The output voltage on the third digital voltmeter will then be near 1.000 per revolution of the probe about the $\emptyset$ axis. It is recommended that R_1, R_2, and R_3 be each a combination of a fixed resistor smaller than the above quoted values and a potentiometer in series for adjusting the total resistances of R_1, R_2, and R_3 to the exact value required for the above quoted outputs per revolution of the probe or the two screws. The positions of the screws and probe will then be read directly on the 3 digital voltmeters indicated on Figure 7, provided that the slide positions on R_4, R_5, and R_6 are adjusted so that each of the voltmeters reads zero when the probe is at the zero reference on the $\emptyset$ axis and the probe linkage is in

the right-angled position indicated in Figure 3. (The values of R_4, R_5, and R_6 should each be 10,000 ohms.) For economy, the three digital voltmeters may be, of course, replaced by a single digital voltmeter and a three position switch.

Because the two screws are driven through rubber couplings which have a small amount of backlash, the two screws should always be driven in just one direction before attempting to stop at a precise point. The preferred direction is a clockwise rotation of the screws (as seen in Figure 2), which corresponds to a positive change in x_1 and a negative change in y_1; this requires a positive voltage at terminal A (Figure 7) and a negative voltage at terminal C.

Care must be exercised to avoid over-running the probe limits of travel and resultant probe damage. The Ø travel is protected by two small limit switches. The x_1 and y_1 travel does not have limit switches; furthermore, care must be taken to avoid breaking either of the two hot wires by contact with the opposite probe tip. Also, the number 1 and 2 potentiometers can be damaged by over-running their travel limits. These potentiometers have a turn limit of only 10 turns, which corresponds to 25 turns of the motor output shafts. If the R_4 and R_5 sliders are moved to the end nearest to pin 1, the digital voltmeters will read a voltage that goes to near zero as the probe potentiometers are turned toward one end of their travel, and to near 2.500 V as the probe potentiometers are turned toward the opposite end of their travel. This test will serve to define the limits of travel without injuring the probe potentiometers.

If desired, three switches may be added in the wires going to the three slider arms of R_4, R_5, and R_6 so that these wires may be switched to pin 1 of the Cannon plug. This will permit testing for the limits of the probe potentiometer without disturbing the slider adjustments on R_4, R_5, and R_6.

SECTION 3

PROBE TIP AND HOT-WIRE CONSTRUCTION

A schematic view of the probe tips have been given in Figure 3; the tips are also visible in Figure 1. An enlarged view of one probe tip is shown in Figure 8. The tip unplugs from the main part of the probe so that the hot-wire element may be easily inspected or modified. The two phosphor-bronze wires or "needles" form the male part of the plug, and the needles extend through to the hot-wire end of the tip. At this end the needles are tapered to a diameter of 0.010 in. The distance ℓ between the needles is varied according to the application.

The needles may be bent or distorted so that the relative position of the two hot-wires may be varied to suit a particular application. The upper part of Figure 9 illustrates a pair of probe tips operated in the normal manner, but with some curvature near the needle tips so that the hot wires may be aligned with the stream without interference between the two tips. The lower part of Figure 9 illustrates a second pair of

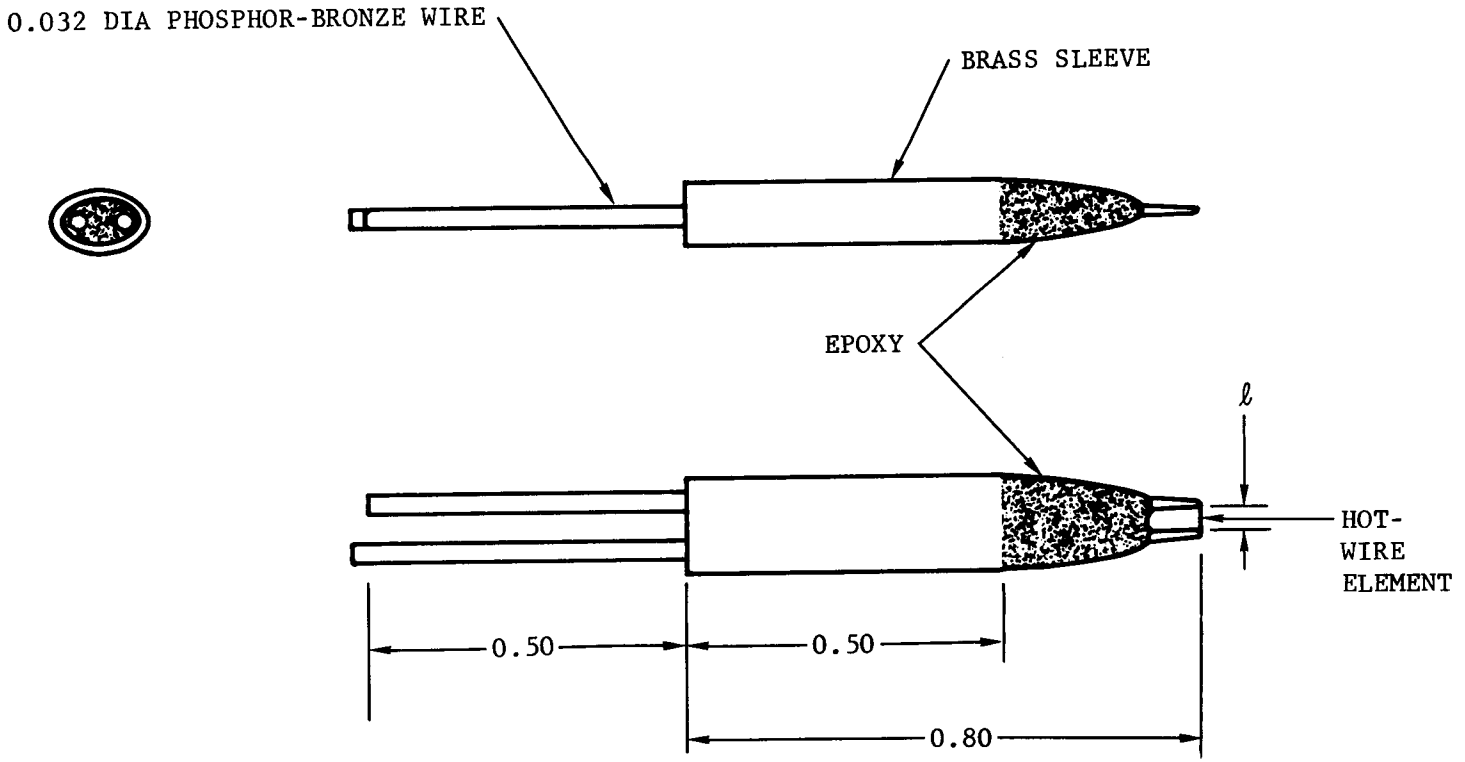

FO4927 U

FIGURE 8. PROBE TIP AND HOT-WIRE ELEMENT

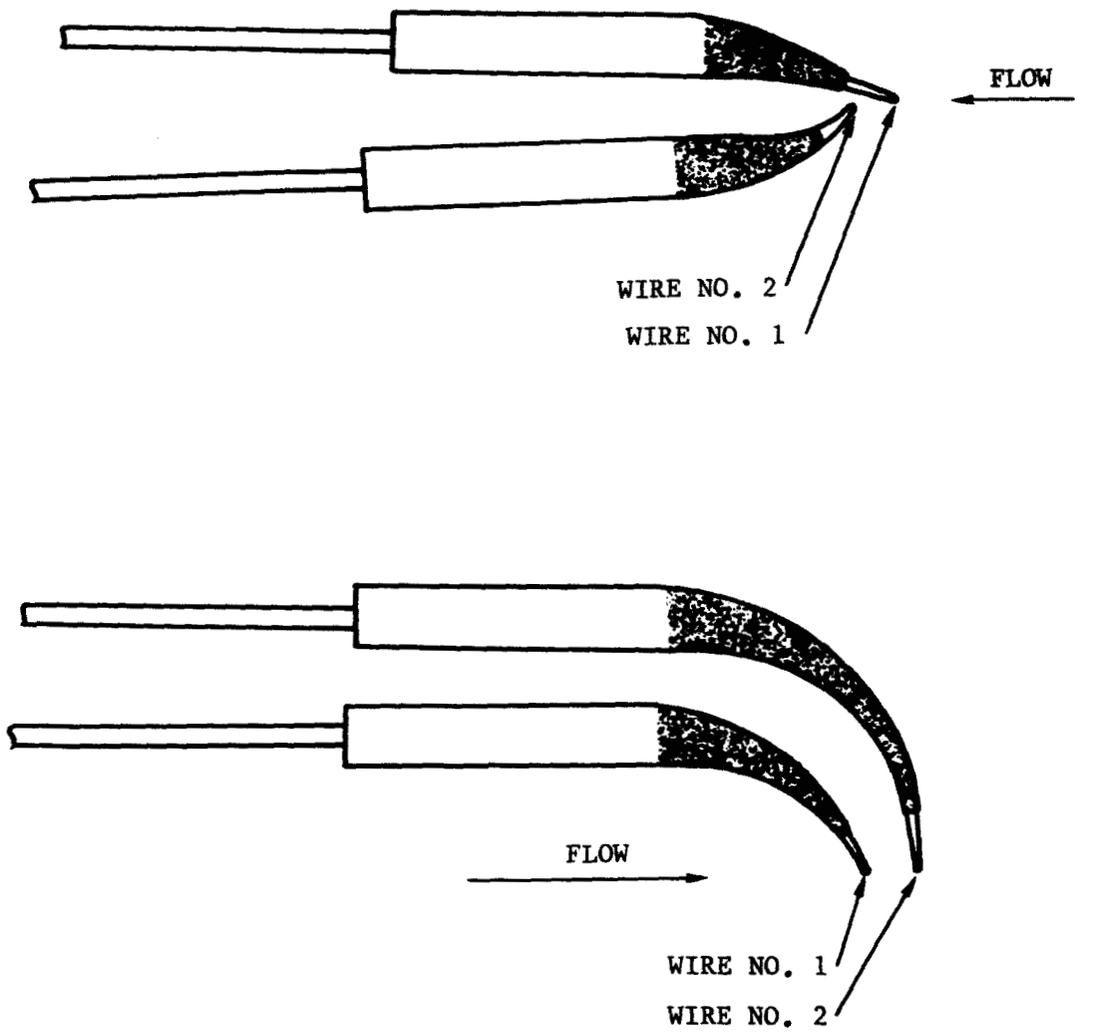

FIGURE 9. EXAMPLES OF PROBE TIP CONFIGURATIONS

tips which were constructed especially to measure a region of reverse flow. Such a configuration was used for the reverse flow measurements reported in Section 7. Note that in this case the roles of wire 1 and wire 2 are interchanged from those indicated by Figure 3. This interchange is possible by interchanging the pulse generator and the control circuit terminals of Figure 7.

Best results in both the subsonic and supersonic tests were had using a wire 1 diameter of 0.0003 in. and a length ℓ (Figure 8) of near 0.060 in. For wire 2 the best results were obtained with a diameter of 0.00010 in. and ℓ = 0.015 in. These dimensions permitted the no. 2 tip to fit between the needles of the no. 1 tip if desired for ease in aligning the wires with the stream. A second advantage of this is that the no. 2 wire tends to stay out of the wake of the needles supporting the no. 1 wire.

If wire no. 1 is made of a smaller diameter, the above advantages are lost because of the necessarily shorten length of the wire. If the no. 1 wire is made larger, the Hewlett-Packard 214A pulse generator used to drive the wire is no longer powerful enough to fully heat the wire during one pulse. Wire no. 2 cannot be made much larger without destroying the above advantages; if it is made much smaller the wire tends to be fragile and difficult to mount on the probe tip.

For all tests the wire material was 90% Pt and 10% Rh. The wire was purchased from the Sigmund Cohn Corporation of Mt. Vernon, N.Y. As purchased, the wire was coated with silver for ease in handling. The

wires were mounted onto the probe tip needles by first removing an inch or less of wire from its spool and attaching it with a bit of wax to the end of a 0.035 in dia copper wire. The copper wire, which was about 2 inches long, had its opposite end permanently attached to a three ounce brass weight which rested flat on the work-table top. The copper wire could then be bent so that it would hold the Pt-Rh wire to rest against the probe needles.

Before the wire was soldered in place, the needles were thoroughly tinned with a thin coating of a good grade of solder. Rosin flux was used to clean the needles; also a little flux was placed on the needles to help hold the wire in place.

The probe tip and needles was held by a small holder mounted in a bench vise. The relative position of the needles and the wire was observed either by the naked eye or by a stereo microscope having a 20X magnification. Before soldering, the silver coating on the last 1/16 in. or so of the wire was removed by immersion of the wire tip in a warm 50% HNO_3 bath. Then the wire position was carefully adjusted with respect to the needle tips. Finally, the tip of a small iron was used to press the wire against each of the two needles. Careful manipulation of the iron would tend to wrap the wire around the needle tip and result in a strong joint. The solder surface tension aided in holding the wire in place until the solder cooled. After the wire attachment, a razor blade was used to remove the unused portion of the wire from the needle tips. The remaining piece of coated wire could then be used for several other probe tips before it was necessary to cut a new length of wire.

Other aids to the wire mounting process include a small "Tensor" lamp to provide good illumination of the wire, a two-inch square of black non-glossy paper, and a small platform for holding the vise. The Tensor lamp could be located so that a bright reflection shone off the wire; the black paper provided a good background so that the wire could be observed even more clearly. The platform, which was only one-half inch in height, had a small adjustment screw which changed the height of one end of the platform. This adjustment permitted the needles to be moved upward or downward by 0.001 in or more at a time to aid in placing the needles at the proper height with respect to the wire.

By using the above procedures, the hot wires were sufficiently well-joined to the needles that wire breakage from the peak air loads of tunnel startup or shutdown was all but eliminated.

Recently, a 92% Pt and 8% W wire has become available (#479 Platinum, Sigmund Cohn Corp.) in diameters as small as 0.0002 in. This wire is almost 3 times as strong as the 90% Pt and 10% Rh wire, and its resistivity is almost twice as large as the previous wire. This means that the new wire, when used in place of the above no. 1 wire, should absorb almost twice the heat for a given setting of the pulse generator output; furthermore, its added strength may withstand the higher heating rate. The result should be an amplified heat signal.

The second wire should not use the 92% Pt - 8% W alloy, since the material thermal coefficient of resistance is quite small.

SECTION 4

VELOCITY MEASUREMENT TESTS IN SUBSONIC FLOW

The second progress report[4] and other sources[1,2] have described subsonic velocity measurements using the two-wire probe. The probe was placed in a small, subsonic wind tunnel. The first wire was heated by connecting its terminals directly to the output of a Hewlett-Packard 214A Pulse Generator. The second wire was heated with a steady current, and the wire voltage fluctuations were amplified using a Transmetrics hot-wire amplifier. The amplifier output was displayed on an oscilloscope whose trace was triggered by the pulse generator.

4.1 PULSE LENGTH AND AMPLITUDE

Throughout the testing, the pulse length and amplitude was varied over a wide range.[4,5] Best results were obtained with a pulse length of 5 microseconds. Shorter times did not heat the wire efficiently,[5] whereas longer times tended to complicate the measurement of t_o. The amplitude was kept as large as adequate wire life would permit; on most tests, which

used the 0.0003 in wires discussed in Section 3, the Hewlett-Packard 214A generator was switched to the maximum output available on the 50 volt scale.

The pulse repetition rate was varied from 10 per second to 167 per second. The lowest rate, 10 per second, was generally the most satisfactory since this allows the maximum time for the first wire to cool between pulses. This low rate had the advantage of increasing the lifetime of the first wire.

4.2 SECOND WIRE CURRENT AND SIGNAL AMPLIFICATION

The second wire current was varied over a wide range.[4,5] A current level of 10 ma was found to be satisfactory for all the testing, assuming a second wire diameter of 0.00010 in as discussed in Section 3. The amplifier was used with the compensation unit switched out, and with the high and low pass filters set at 10 cps and 320 kcps, respectively. The amplifier and oscilloscope gain settings were adjusted so that the second wire signal amplitude was large enough to be conveniently viewed on the screen. Typical gain settings were 12,000 on the amplifier and 2 volts/cm on the oscilloscope.

4.3 OSCILLOSCOPE SCREEN DISPLAY

The first and second wire voltages were displayed on a dual-beam oscilloscope; a schematic diagram of the display is shown in Figure 10. The second wire trace is displayed in the lower half of the figure; the sloping portion of the trace is the result of the heat pulse produced by

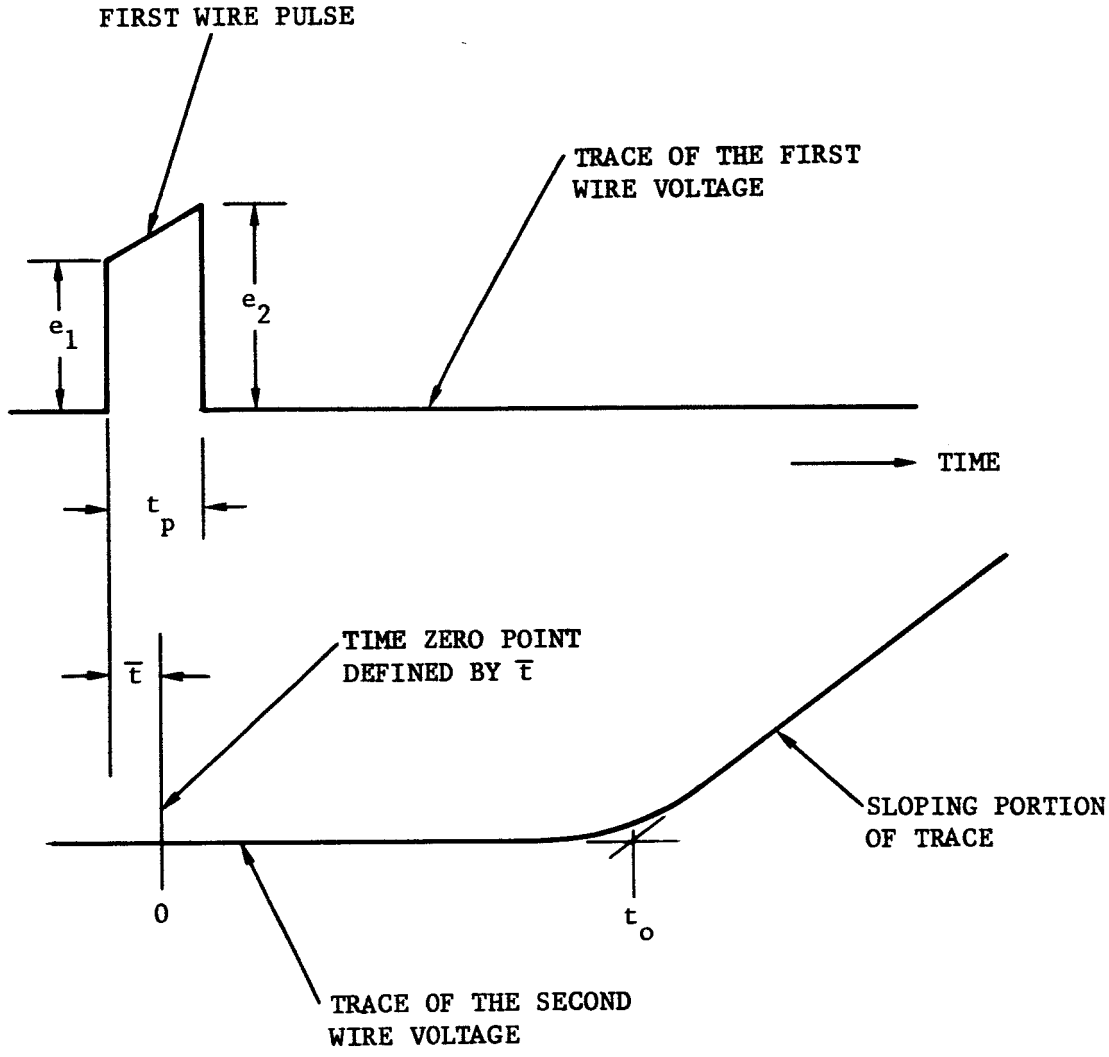

FO4928 U

FIGURE 10. SCHEMATIC DIAGRAM SHOWING THE ESSENTIAL FEATURES OF THE HOT-WIRE VOLTAGES AS DISPLAYED ON THE OSCILLOSCOPE SCREEN

the first wire. The second wire temperature increases at a rate almost exactly proportional to the magnitude of the heat pulse. Since the second wire current is a constant, the lower trace (Figure 10) varies in amplitude like the wire resistance, which is a linear function of the wire temperature. Therefore, the lower trace is really a measure of the second wire temperature. Because the leading edge of the heat pulse diffuses, as explained in References 1 and 2, the corner near t_o on the lower trace is rounded. However, the sloping portion of the lower trace is not significantly affected by the diffusion, as explained in References 1 and 2. The time t_o is measured to the point of intersection of the sloping portion of the trace and the horizontal portion of the lower trace.

The time origin for measuring t_o is defined by the center of gravity of the energy input to the first wire. The energy input is defined by e_1, e_2, and t_p shown on the figure plus the assumption of constant current from the pulse generator. This assumption is justified because the wire resistance of the wires discussed in Section 3 is small compared to the output impedance of the Hewlett Packard 214A generator. Then the time origin may be shown to be at time $\bar{t}$ later than the leading edge of the pulse, where $\bar{t}$ is given by

$$\bar{t} = t_p \left(\frac{1 + \frac{2k}{3}}{2 + k}\right) \qquad (4\text{-}1)$$

where

$$k = \left(\frac{e_2}{e_1} - 1\right) \qquad (4\text{-}2)$$

This calculation also depends on the assumption that the voltage pulse is linear in time between the limits e_1 and e_2. However, small departures from linearity, as given by the temperature resistance character of Pt - 10% Rh wires, are not significant. For values of k between 0 and ∞, the ratio $\bar{t}/t_p$ varies from 1/2 to 2/3; for values of k close to 1/2, which is typical of the experiments to date, the ratio $\bar{t}/t_p$ is 0.533. This is very little different from 0.500, and such differences are significant for high speed measurements such that t_o is less than 2 or 3 times t_p. For the subsonic tests, t_o is much larger than t_p, so that the errors involved in assuming $\bar{t}$ to be 1/2 t_p have been negligible.

The time t_o is the time required for the heat transferred from the first wire to travel to the second wire, assuming zero heat diffusion in the airstream. The heat diffusion is the reason for the rounding of the corner of the lower trace in Figure 10, and the fact that the first wire is heated over a finite length of time (t_p) rather than instantaneously has complicated the measurement of t_o.

4.4 EFFECT OF WIRE NO. 1 WAKE ON t_o

The discussion of Figure 10 has served to demonstrate the measurement of t_o from the oscilloscope screen. The following will show how t_o is used to determine the stream speed U.

Because wire 1 may slow down the heat transit through the velocity defect of its wake, the assumption that U equal x_o/t_o, as used in References 1 and 2, cannot be justified. Instead, use is made of Reference 6 to obtain the velocity defect far behind a streamwise flat

plate. When the plate is replaced by a cylinder of diameter d such that the drag force is the same as on the plate, the velocity defect in the far wake is unchanged. The defect along the wake centerline may be calculated easily and is, in terms of the cylinder,

$$(U - u) = \frac{A_1 U}{(\frac{x}{d})^{\frac{1}{2}}} \qquad \text{("far" wake only)} \qquad (4\text{-}3)$$

where $$A_1 = \frac{C_D}{4} (\frac{R_d}{\pi})^{\frac{1}{2}} \qquad (4\text{-}4)$$

$$R_d = \frac{\rho U d}{\mu} \qquad (4\text{-}5)$$

U is the free stream speed, and the cylinder drag coefficient C_D may be given as a function of Reynolds number R_d and Mach number M, as in Figure 1.4 of Reference 6.

Since we do not have an analytic solution for u in the near wake immediately behind the first wire, we must make some estimate of this velocity. Here we will assume that

$$u = B_1 U \qquad \text{("near" wake only)} \qquad (4\text{-}6)$$

where B_1 is a parameter that may be adjusted to fit the experimental data. This assumes u to be constant in the near wake, which should be adequate for the following calculations.

The junction of the near and far wakes will be here defined as the point where equations (4-3) and (4-6) give the same value of u. This is

$$(\frac{x}{d})_j = (\frac{A_1}{1 - B_1})^2 \qquad (4\text{-}7)$$

Then the time of travel of the centerline fluid from wire one to wire two will be

$$t_o = \int_o^{x_o} \frac{dx}{u} \tag{4-8}$$

where u is given by Equation (4-7) for $0 \le (\frac{x}{d}) \le (\frac{x}{d})_j$ and by Equation (4-3) for $(\frac{x}{d})_j \le (\frac{x}{d}) \le (\frac{x_o}{d})$. The length x_o is the distance between the two wires. Equation (4-8) integrates to

$$t_o = \frac{x_o}{Ug(\xi, B_1)} \tag{4-9}$$

where

$$g(\xi, B_1) = B_1 \qquad \text{for } \xi \ge (1 - B_1) \tag{4-10}$$

and

$$g(\xi, B) = \frac{1}{1 + 2\xi + \xi^2\{\frac{1 - 2B_1}{B_1(1 - B_1)} + 2\ell n(\frac{(1 - \xi)(1 - B_1)}{\xi B_1})\}}$$

$$\text{for } 0 \le \xi \le (1 - B_1) \tag{4-11}$$

where $$\xi = \frac{A_1}{(\frac{x_o}{d})^{\frac{1}{2}}} \tag{4-12}$$

Figure 11 gives A_1 as a function of R_d and M. For the case of small Knudsen numbers, Schlichting's Figure 1.4[5] and the Oseen drag law were used to compute A_1. For large values of the Knudsen number,

$$K_{n_\infty} = (\frac{\pi\gamma}{2})^{\frac{1}{2}} \frac{M}{R_d} \tag{4-13}$$

the free-molecular drag formula of Stalder, Goodwin, and Creager was used.[7,8]

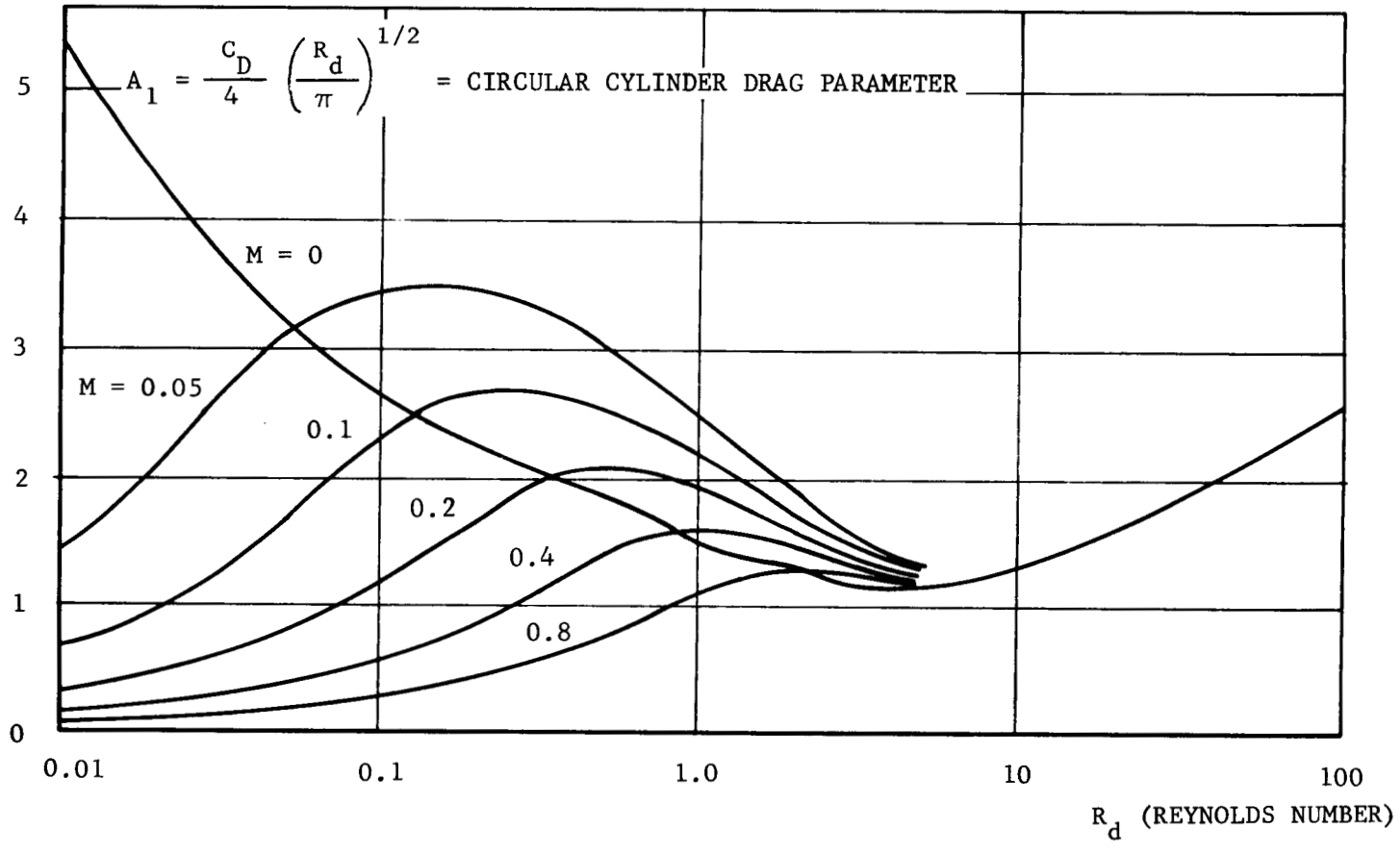

FIGURE 11. A_1 VERSUS R_d AND M

The $\bar{\eta}_*$ factor given by Dewey[9] was used to interpolate between the free-molecule and the continuum flow limits in constructing Figure 11.

Pritts[10] has shown experimentally that the velocity defect becomes greater as the free stream velocity is increased from 50 to 200 feet/sec. This was shown for x_o's between about 0.01 in and 0.10 in and for d's of both 0.0002 in and 0.0004 in. The corresponding values of R_d were 5.2, 10.5, and 21 for the smaller wire and 10.5, 21, and 42 for the larger wire. Reference to Figure 11 shows A_1 increasing with R_d in this region. Therefore, the velocity defect should also have increased with R_d. This expected trend is fully confirmed by Reference 10.

The overall velocity defect results are correlated on Figure 12 in terms of the correlation parameter $\xi = A_1/(x_o/d)^{\frac{1}{2}}$. The velocity defect function $g(\xi, B_1)$, which is just the ratio of the time for the free stream to travel the distance x_o divided by the time taken for the centerline fluid to travel x_o, is shown for $B_1 = 0.2$ and $B = 0.3$. The experimental data correlates best with the $B_1 = 0.2$ line. The data given by Pritts[10] and by the writer appear to correlate equally well. Because of the large volume of the Reference 10 data, many of the points were omitted so that the remainder would be clear; however, all of the Reference 10 data appear to be in good agreement with Figure 12.

4.5 VELOCITY MEASUREMENTS

When correction is made for the velocity defect, by use of $g(\xi, 0.2)$ in the equation

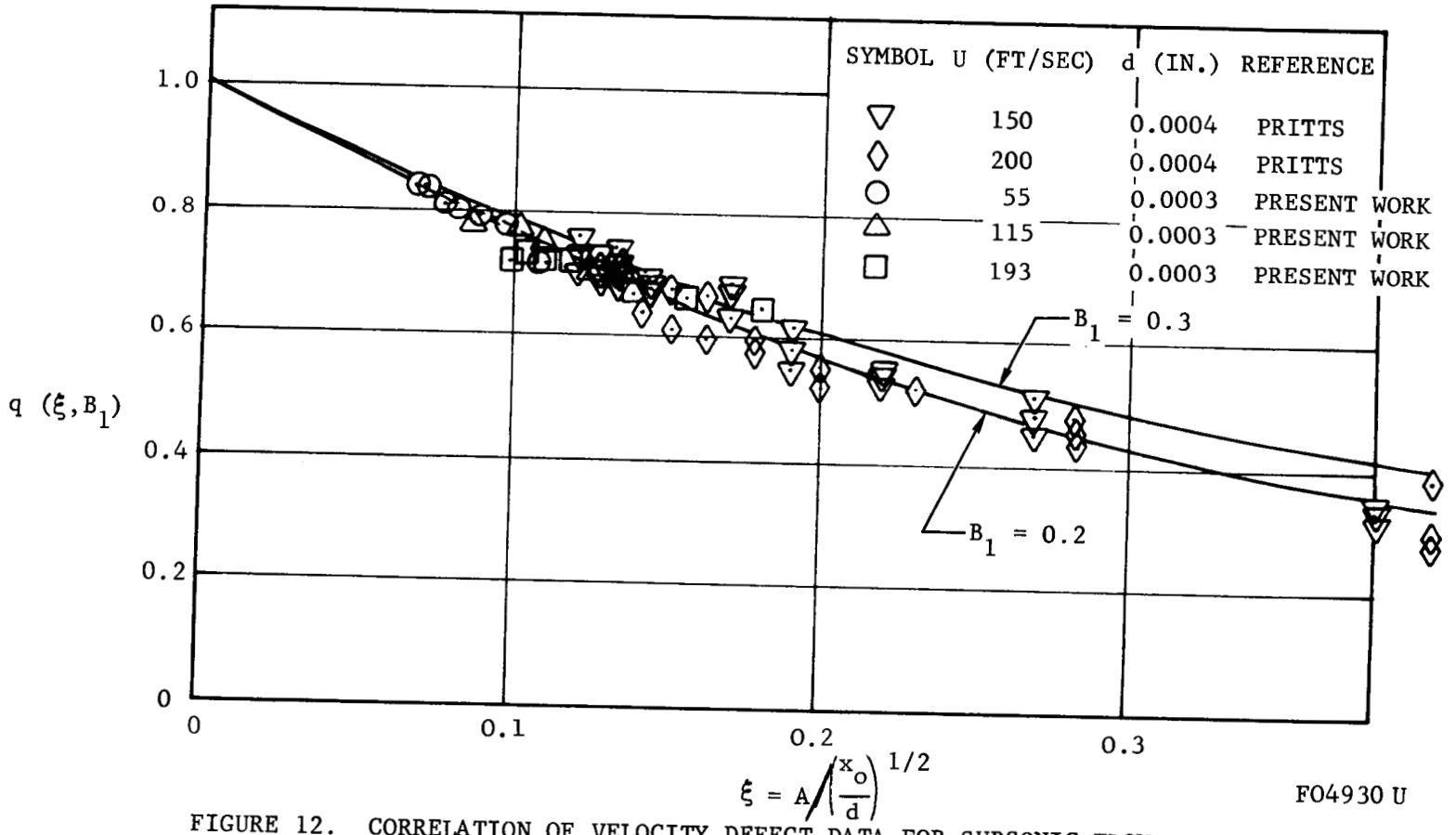

FIGURE 12. CORRELATION OF VELOCITY DEFECT DATA FOR SUBSONIC FLOW SUBSONIC SPEEDS

$$U = \frac{x_o}{t_o g(\xi, 0.2)} \qquad (4\text{-}14)$$

the stream velocity U is obtained. The data points on Figure 12 contain a small amount of scatter; the same degree of scatter may be expected in using the measured t_o to compute U from Equation (4-14). The parameter ξ is obtained from Equation (4-12) and Figure 11. This requires knowledge of R_d and M. Usually these are known approximately; however, Section 6 describes a complete data reduction scheme which determines R_d and M by the use of t_o, x_o, and two hot-wire resistance measurements.

SECTION 5

VELOCITY MEASUREMENT TESTS IN SUPERSONIC FLOW

The fourth progress report[11] has described supersonic velocity measurements using the two-wire probe placed in the test section of the Aeronutronic Mach 3 tunnel. The transit time was measured exactly as described in Section 4 for the subsonic tests. Because t_o was not large compared to t_p in the supersonic testing, Equation (4-1) was used to define $\bar{t}$ in obtaining t_o. The shortness of t_o also created a problem in measuring t_o, since the electrical disturbance generated by the pulse generator in heating wire 1 always was sensed by the wire 2 circuit and was amplified and displayed as an interference or "cross talk" on the second wire oscilloscope trace. This cross talk usually appeared over much of the horizontal part of the second wire trace, as seen in Figure 10. Fortunately, the effect of the cross talk appeared independent of the current in the second wire. With the second wire current at zero, the cross talk effect alone could be observed. This made it possible to

correct the oscilloscope traces for the cross talk. A Polaroid camera was quite useful for recording the oscilloscope traces of both the cross talk alone and the cross talk plus the velocity signal. (For the subsonic measurements, cross talk was not a problem, inasmuch as t_p was much less than t_o.)

For the supersonic case, the velocity defect behind the first wire should be much different from the subsonic case, since a major portion of the cylinder drag is associated with the bow shock wave mechanism. This will spread the velocity defect over a much wider region than in the subsonic case, and the defect may be a much smaller fraction of the free stream speed than in the subsonic case. The problem is sufficiently complex that a measurement of the velocity defect would be required before one could determine its importance to the supersonic case.

In the fourth progress report,[11] the supersonic velocity defect was assumed zero, so that

$$U = \frac{x_o}{t_o} \tag{5-1}$$

The resulting two-wire velocity measurements agreed, within experimental error, with the supersonic velocity determined by pitot and static pressure and the stream total temperature measurements.[11]

For most of the supersonic measurements, x_o was larger than 0.2 in. This large value was necessary in order that t_o be long enough to permit t_o to be measured with fair accuracy. In general, x_o should be long enough that t_o is at least 10 microseconds.

In all other respects, the experimental setup was similar to that for the subsonic tests.

SECTION 6

PROBE DATA REDUCTION METHOD

The two wire probe is capable of measuring five different quantities at or near each point in a flow field. Two of these quantities, $\emptyset$ and θ, relate only to the direction of the velocity vector, and may be dismissed here since they do not interact with the other three in the determination of other flow quantities. The other three - x_o/t_o, e_a, and e_b are used with certain calibration constants to compute the fluid velocity U, pressure p, density ρ, and temperature T. Here e_a and e_b are defined as the voltages across the no. 2 wire and the wire leads for two values, i_a and i_b, respectively, of the wire current.

6.1 HOT-WIRE MEAN TEMPERATURE

Before discussing the data reduction procedure, it is instructive to review the analysis of hot-wire operation so that a

better understanding is obtained for the physical meaning of the wire voltages e_a and e_b and the corresponding wire currents i_a and i_b.

Dewey[12] has written the differential equation which describes the heat transfer from the wire to the airstream and the heat conduction along the wire itself. When this equation is solved for the condition that each end of the wire is at temperature T_s, the wire will be found to have a hyperbolic cosine temperature distribution. When this distribution is integrated over the length of the wire, the mean wire temperature is found to be

$$T_{wm} = H - (H - T_s)\left(\frac{\tanh \nu}{\nu}\right) \tag{6-1}$$

where H is the temperature of an infinitely long wire and ν is a correction parameter for the wire end, which is at temperature T_s. Now,

$$H = \frac{T_* + A(1 - \alpha T_R)}{1 - \alpha A} \tag{6-2}$$

and

$$\nu = \frac{\ell}{d}\left[\left(\frac{k_o Nu_o}{k_w}\right)(1 - \alpha A)\right]^{\frac{1}{2}} \tag{6-3}$$

where the symbols are defined as:

T_* = infinite wire recovery temperature

$$A = \frac{i^2 R_R}{\pi k_o \ell Nu_o} \tag{6-4}$$

i = wire current

R_R = wire resistance at some reference temperature T_R

k_o = fluid thermal conductivity at T_o

T_o = total temperature of the flow

ℓ = wire length

d = wire diameter

N_{uo} = Nusselt number, as defined by Dewey[9,12]

α = resistivity coefficient as used in the following relation for wire resistance

$$R = R_R[1 + \alpha(T_{wm} - T_R)] \tag{6-5}$$

k_w = wire thermal conductivity

Dewey[9,13] has also correlated much cylindrical heat transfer data to show in graphical form Nu_o as a function of Re_o and Mach number M. He also has related $\eta_* \equiv \frac{T_*}{T_o}$ to the Knudsen number

$$K_{n\infty} = (\frac{\gamma\pi}{2})^{\frac{1}{2}} \frac{M}{Re_\infty} \tag{6-6}$$

where $$Re_o = \frac{\rho U d}{\mu_o} \text{ and } Re_\infty = \frac{\rho U d}{\mu_\infty} \tag{6-7}$$

where μ_o is the viscosity at temperature T_o; μ_∞ is the viscosity at the static temperature T; and γ is the ratio of specific heats of the gas. Finally, if the leads going to the hot wire have some resistance, R_L, the wire voltage can be written as

$$e = i(R + R_L) \tag{6-8}$$

With the above relations, it is a simple problem in substitution to compute e when given values of i, U, p, ρ, and T plus the wire parameters k_w, ℓ, d, α, and R_R and the fluid parameters γ, k_o, and μ_o.

A more difficult problem is to compute p, ρ, T and U when given the five measurements x_o/t_o, e_a, and e_b, i_a, and i_b plus the above parameters. The steps for this calculation, which involves an iteration procedure, are given below in Section 6.2. The procedure makes use of the above equations.

The voltages e_a and e_b may be used to calculate the corresponding values of wire resistance

$$R_a = e_a/i_a - R_L \tag{6-9}$$

$$R_b = e_b/i_b - R_L \tag{6-10}$$

and wire mean temperature

$$T_{wm_a} = \frac{R_a - R_R}{\alpha R_R} + T_R \tag{6-11}$$

$$T_{wm_b} = \frac{R_b - R_R}{\alpha R_R} + T_R \tag{6-12}$$

If i_a is almost zero, A_a will be so small that H_a (Equation (6-2)) is almost equal to T_{*_a}. If the wire aspect ratio ℓ/d is sufficiently large, the end correction in Equation (6-1) will be small so that T_{wm_a} is almost equal to both H_a and T_{*_a}. Dewey[9,12,13] has shown that T_* is almost equal to T_o, so that T_{wm_a} gives an approximate measure of T_o.

On the other hand, for $i = i_b$ sufficiently large that A_b is of the order of 100^oR, both H_b and T_{wm_b} will be significantly larger than T_* or T_o. Now, the wire Nusselt number is given by

$$Nu_o = \frac{i^2R}{\pi k_o \ell (T_w - T_*)} \tag{6-13}$$

for an infinitely long wire at temperature T_w losing heat at the rate i^2R. Therefore, if we can neglect wire end effects,

$$Nu_o \approx \frac{i_b^2 R_b}{\pi k_o \ell (T_{wm_b} - T_{wm_a})} \tag{6-14}$$

is an approximate value of Nu_o, where k_o is evaluated at T_{wm_a}. From the speed x_o/t_o and the speed of sound defined by T_{wm_a}, Mach no. is easily computed. By using Nu_o and M with Dewey's curves, Re_o may be obtained. From this, ρU is easily found.

Therefore, the five measurements e_a, e_b, i_a, i_b, and x_o/t_o may be used to readily obtain approximate values of ρU, U, and T_o, as was originally suggested on page 17 of Reference 1. From these, it is easy to compute approximate values of p, ρ, and T.

The next section, 6.2, gives a procedure much like the above to calculate by an iteration procedure more precise values of the stream variables.

6.2 DATA REDUCTION PROCEDURE

The following steps are used for the data reduction procedure:

1. Use equations (6-9) to (6-12) to compute R_a, R_b, T_{wm_a}, and T_{wm_b}.

2. T_{01} is the first approximation to T_o. (Other subscripts 1,2,3, ... represent similar approximations.)

$$\text{Let } T_{01} = T_{wm_a} \tag{6-15}$$

3. $$k_{01} = k_o\,(T_{01}) \tag{6-16}$$

Note: for air, the following table lists values of k_o:

$T(^oK)$	$k_o \times 10^4$ (watts/inch/^oK)
80	1.897
90	2.120
100	2.348
120	2.806
140	3.261
160	3.712
180	4.155
200	4.595
220	5.030
240	5.450
260	5.865
280	6.260
300	6.665
320	7.060

4. $$N_{u_{01}} = \frac{0.8\, i_b^2\, R_b}{\pi K_{01}\, \ell\, (T_{wmb} - T_{wma})} \qquad (6\text{-}17)$$

5. $$\nu_1 = \frac{\ell}{d}\left[\left(\frac{K_{01}}{K_w}\right) N_{u_{01}}\right]^{\frac{1}{2}} \qquad (6\text{-}18)$$

6. $$N_{u_{02}} = \frac{N_{u_{01}}}{0.8}\left(1 - \frac{\tanh \nu_1}{\nu_1}\right) \qquad (6\text{-}19)$$

7. $$\nu_2 = \frac{\ell}{d}\left[\left(\frac{K_{01}}{K_w}\right)\left(N_{Nu02}\right)\left(1 - \frac{\alpha\left(T_{wmb} - T_{wm3}\right)}{1 - \left(\frac{\tanh \nu_1}{\nu_1}\right)}\right)\right]^{\frac{1}{2}} \qquad (6\text{-}20)$$

8. $$N_{Nu03} = \frac{N_{Nu01}}{0.8}\left(1 - \frac{\tanh \nu_1}{\nu_2}\right) \qquad (6\text{-}21)$$

9. $$U_1 = \frac{X_0}{t_0} \qquad (6\text{-}22)$$

10. Solve for M_1:

$$\frac{M_1}{\left(1 + \frac{\gamma - 1}{2} M_1^2\right)^{\frac{1}{2}}} = \frac{U_1}{\left(\gamma \mathcal{R} T_{01}\right)^{\frac{1}{2}}} \qquad (6\text{-}23)$$

where $\mathcal{R}$ is the gas constant in the equation of state

$$P = \rho \mathcal{R} T \qquad (6\text{-}24)$$

11. $$R_{e01} = R_{e0}\left(N_{Nu03}, M_1\right)$$

Find this from Dewey's Chart.[13]

12. If above M_1 is greater than 1, let $U_2 = U_1$. If it is less than 1, use M_1 and Re_{01} to compute $g(\xi, 0.2)$ as described in Section 4. Then compute

$$U_2 = \frac{U_1}{g(\xi, 0.2)} \qquad (6\text{-}25)$$

and use U_2 in place of U_1 to recompute steps 10 and 11.

13. $$T_1 = \frac{T_{01}}{1 + \frac{\gamma - 1}{2} M_1^2} \qquad (6\text{-}26)$$

14. $$K_{n_{\infty 1}} = \left(\frac{\gamma \pi}{2}\right)^{\frac{1}{2}} \frac{M_1}{Re_{01}} \frac{\mu(T_1)}{\mu(T_{01})} \qquad (6\text{-}27)$$

where $\mu(T)$ is, for air,

$$\mu = 2.270 \frac{T^{3/2}}{T + 198.6} \times 10^{-8} \quad \frac{lb\ sec}{ft^2} \qquad (6\text{-}28)$$

(Sutherland's formula) (for T in °K

15. $$\eta_{*_1} \equiv \frac{T_{*1}}{T_c} = \eta_* (K_{n_{\infty 1}}) \qquad (6\text{-}29)$$

as given by Dewey.[13]

16. $$A_{21} = \frac{i_2^2 R_R}{\pi \ell \lambda_{01} Nu_2} \qquad (6\text{-}30)$$

17. $$\nu_{a2} = \frac{\ell}{d} \left[\left(\frac{K_{01}}{K_w}\right) (Nu_{02}) (1 - \alpha A_{21}) \right]^{\frac{1}{2}} \qquad (6\text{-}31)$$

18. $$\omega_{21} = \frac{\nu_{a2}}{\tanh \nu_{a2}} \qquad (6\text{-}32)$$

19. $$\eta_{s_1} = \frac{T_s}{T_{01}} \qquad (6\text{-}33)$$

Dewey[12] discusses η_s and recommends the value 0.903 for $M < 1$. For $M > 1$, use $\eta_s = 1.000$.

20. $$T_{02} = \frac{\left(\frac{\omega_{21} T_{wm2}}{\omega_{21} - 1}\right)(1 - \alpha A_{21}) - A_{21}(1 - \alpha T_R)}{\eta_{*_1} + \left(\frac{\eta_{s1}}{\omega_{21} - 1}\right)(1 - \alpha A_{21})} \qquad (6\text{-}34)$$

21. $T_{*1} = \eta_{*1} T_{02}$ (6-35)

22. $\omega_{b1} = \frac{\nu_2}{\tanh \nu_2}$ (see step 7) (6-36)

23. $H_{b1} = \frac{\omega_{b1} T_{wmb} - \eta_s T_{02}}{\omega_{b1} - 1}$ (6-37)

24. $R_{Hb} = R_R \left[1 + \alpha (H_{b1} - T_R)\right]$ (6-38)

25. $k_{02} = k_0 (T_{02})$ (6-39)

26. $Nu_{04} = \frac{i_b^2 R_{Lb}}{\pi k_{02} \ell (H_{b1} - T_{*1})}$ (6-40)

27. Solve for M_2:

$$\frac{M_2}{\left(1 + \frac{\gamma-1}{2} M_2^2\right)^{\frac{1}{2}}} = \frac{U_2}{(\gamma R T_{02})^{\frac{1}{2}}} \quad (6\text{-}41)$$

28. $R_{eo2} = R_{eo}(Nu_{04}, M_2)$ (6-42)

see Dewey's chart.[13]

29. If $M_2 > 1$, let $U_3 = U_2$. If $M_2 < 1$, use M_2 and R_{eo2} to compute $g(\xi, 0.2)$ as described in Section 4. Then compute

$$U_3 = \frac{U_1}{g(\xi, 0.2)} \quad (6\text{-}43)$$

and use U_3 to recompute steps 27 and 28.

30. Repeat steps 13 through 21 using latest values of the parameters to compute the next approimxations; i.e.: compute T_2, $K_{n\infty_2}$, η_{*_2}, A_{a2}, ν_{a3}, ω_{a2}, η_{s2}, T_{03}, and T_{*2}.

31. $$A_{b2} = A_{a2} \left(\frac{i_b}{i_2}\right)^2 \tag{6-44}$$

32. $$\nu_{b2} = \frac{\ell}{d}\left[\left(\frac{k_{02}}{K_w}\right)(Nu_{04})(1 - \alpha A_{b2})\right]^{\frac{1}{2}} \tag{6-45}$$

33. $$\omega_{b2} = \frac{\nu_{b2}}{\tanh \nu_{b2}} \tag{6-46}$$

34. $$H_{b2} = \frac{\omega_{b2} T_{wmb} - \eta_{s2} T_{03}}{\omega_{b2} - 1} \tag{6-47}$$

35. $$R_{Hb2} = R_R \left[1 + \alpha (H_{b2} - T_R)\right] \tag{6-48}$$

36. $$K_{03} = K_o (T_{03}) \tag{6-49}$$

37. $$Nu_{05} = \frac{i_b^2 R_{Hb2}}{\pi K_{03} \ell (H_{b2} - T_{*2})} \tag{6-50}$$

38. Solve for M_3:

$$\frac{M_3}{(1 + \frac{\gamma-1}{2} M_3^2)^{\frac{1}{2}}} = \frac{U_3}{(\gamma \mathcal{R} T_{03})^{\frac{1}{2}}} \tag{6-51}$$

39. $$R_{e03} = R_{es}(Nu_{05}, M_3) \tag{6-52}$$

40. If $M_3 > 1$, let $U_4 = U_3$. If $M_3 < 1$, use M_3 and Re_{o3} to compute $g(\xi, 0.2)$ as described in Section 4. Then compute

$$U_4 = \frac{U_1}{g(\xi, 0.2)}$$

and use U_4 to recompute steps 38 and 39.

41. Let $T_0 = T_{03}$ (6-53)

$M = M_3$ (6-54)

$U = U_4$

and $Re_o = Re_{o3}$ (6-55)

42. $$T = \frac{T_o}{\left(1 + \frac{\gamma - 1}{2} M^2\right)}$$ (6-56)

43. $$\mu_o = \mu(T_o)$$ (6-57)

see Equation (6-28).

44. $$\rho = \frac{Re_o \mu_o}{U d}$$ (6-58)

45. $$p = \rho R T$$ (6-59)

The above procedure has been programmed into a Philco computer and used for the data reduction example of Section 7. Also, steps 30 through 40 are iterated two more times to obtain added accuracy. The computer can reduce 100 data points in 2 minutes for a cost of approximately 20 dollars.

The computer has also been programmed for an exact (no iterations required) computation of e_a and e_b using i_a, i_b, p, ρ, T, and U as inputs. This has served to check the accuracy of the data reduction procedure. This check is still underway with each new case fed to the computer. To date, the procedure has been entirely satisfactory.

6.3 DETERMINATION OF HOT-WIRE CALIBRATION CONSTANTS

Wire parameters ℓ, d, k_w, α, and R_R must be known for the proper reduction of the data. For d, we have relied on the wire manufacturer's specification of the diameter, as actual measurement of the diameter would be extremely difficult. Dewey[9,13] has also relied on the manufacturer for d. To determine ℓ, the wire cold resistance has been measured and divided by the manufacturer's quoted value of resistance in ohms per foot. The resulting length agrees well with a direct measurement of wire length. A value k_w = 0.785 watts/in ^{o}K has been used for all computations.

To determine α and R_R, the preferred method has been to place the wire in the supersonic tunnel test section where p, ρ, T, and U are known from the tunnel calibration, as measured accurately by pitot and static pressure measurements and the known tunnel total temperature. Then e_a, e_b, i_a, and i_b are measured; usually i_a is set at 1 ma and i_b at about 8 ma. With these measurements, the equations of Section 6.1 are solved, by computer, to determine the unique values of α and R_R which fit the measurements.

Dewey[12] describes a small furnace which he used to determine α and R_R. This was done by measuring the wire resistance as a function of

temperature, and then using equation (6-5) to find α and R_R. While this method is a correct one, it is believed not to be nearly as satisfactory as the wind tunnel method. This is because the wind tunnel method operates so that any errors in the values of ℓ, d, k_w, η_s, etc. are at least partially compensated.

The wind tunnel method has been used for the results reported in Part 1 of Reference 14. Part 2 of Reference 14 uses a simplified form of the wind tunnel method. This simplification is possible because the flow field does not contain Mach numbers less than about 2.

6.4 USE OF PITOT AND STATIC TUBES IN FLOW FIELD MEASUREMENTS

Although the two-wire method may be used to determine the stream variables, pitot and static tube methods are often faster and more precise. This is true in particular where high-speed velocity measurements in highly turbulent flows are desired. However, pitot and static tube measurements alone are not sufficient for measuring stream variables; also required is the hot-wire determination of stream total temperature by the measurement of e_a and i_a.

Reference 14 uses two different groups of measurements:

Group 1: static and pitot pressures, e_a, i_a

Group 2: static pressure, e_a, i_a, e_b, i_b

Each of these is sufficient to determine the stream variables. These groups do not measure the local stream direction. Therefore, the two-wire method must be used to determine the stream direction.

Section 3.1 of Reference 1 suggests the use of static and pitot probes as an aid in flow field measurements. A logical conclusion is that both the two-wire probe and the pressure instruments should be used, each to its fullest advantage, in flow field measurements.

This has been done in Reference 14, which is believed to be the only example in the literature of the determination of stream variables based entirely on measurements throughout a compressible flow field. Dewey[9] had previously determined stream variables in a like manner, but only in a limited portion of a flow field.

SECTION 7

EXAMPLE OF THE FLOW FIELD MEASUREMENT BEHIND A CONE

Flow field parameters have been measured along a line one-half a base diameter behind a 12 degree half-angle cone. The forward end of the cone was mounted on a streamwise rod which extended through the throat of the Aeronutronic Mach 3 tunnel.[14] Detailed flow measurements of the same field but not using the two-wire probe have been reported elsewhere.[14] The cone base diameter was one inch, the free stream Reynolds number based on base diameter was 112,000, and the Mach number of the free stream was 3.035. The tunnel total temperature was 298.6^{o}K, and the total pressure was 450 mm Hg. The cone was at zero angle of attack.

Because the model was axisymmetric, the flow field was essentially axisymmetric. This fact eliminated the need to rotate the probe about the $\emptyset$ axis in order to bring the wires perpendicular to the stream. All measurements were made in the XY plane, which was vertical and passed through the cone centerline.

7.1 VELOCITY VECTOR DIRECTION MEASUREMENTS

The flow direction measurements are shown on Figure 13. The cone is outlined on the left side of the figure. The arrows represent the measured flow directions; the dots indicate the points to which the measurements refer. The lower three points show the reverse flow region near the axis. The upper 13 points show the flow inclination of the cone expansion fan.

The three lower points were taken with x_o = 0.028 in. Since the flow Reynolds number was quite low, the flow direction measurements were not sharp, and the flow direction was obtained only approximately.

For the upper 13 points the Reynolds number was much larger and the measurements were quite sharp; the flow angle could be determined to within less than one degree. The distance x_o was 0.150 in.

All the measurements were repeated without difficulty as a check on the work. The second wire was always moved to both sides of the heated wake of the first wire to aid obtaining the best possible measure of the flow direction.

7.2 STREAM VARIABLE MEASUREMENTS AND DATA REDUCTION

Figures 14 and 15 show the stream parameters, p, ρ, and T normalized by the corresponding free stream parameters, p_∞, ρ_∞, and T_∞. The free stream values were p_∞ = 0.225 psia, $\rho_\infty = 0.998 \times 10^{-4}$ slugs/ft^3, and $T_\infty = 105.0^\circ$K. U is given in feet/sec. The solid lines were determined from Group 1 measurements - p, p_o' (pitot pressure), e_a, and i_a; the dotted

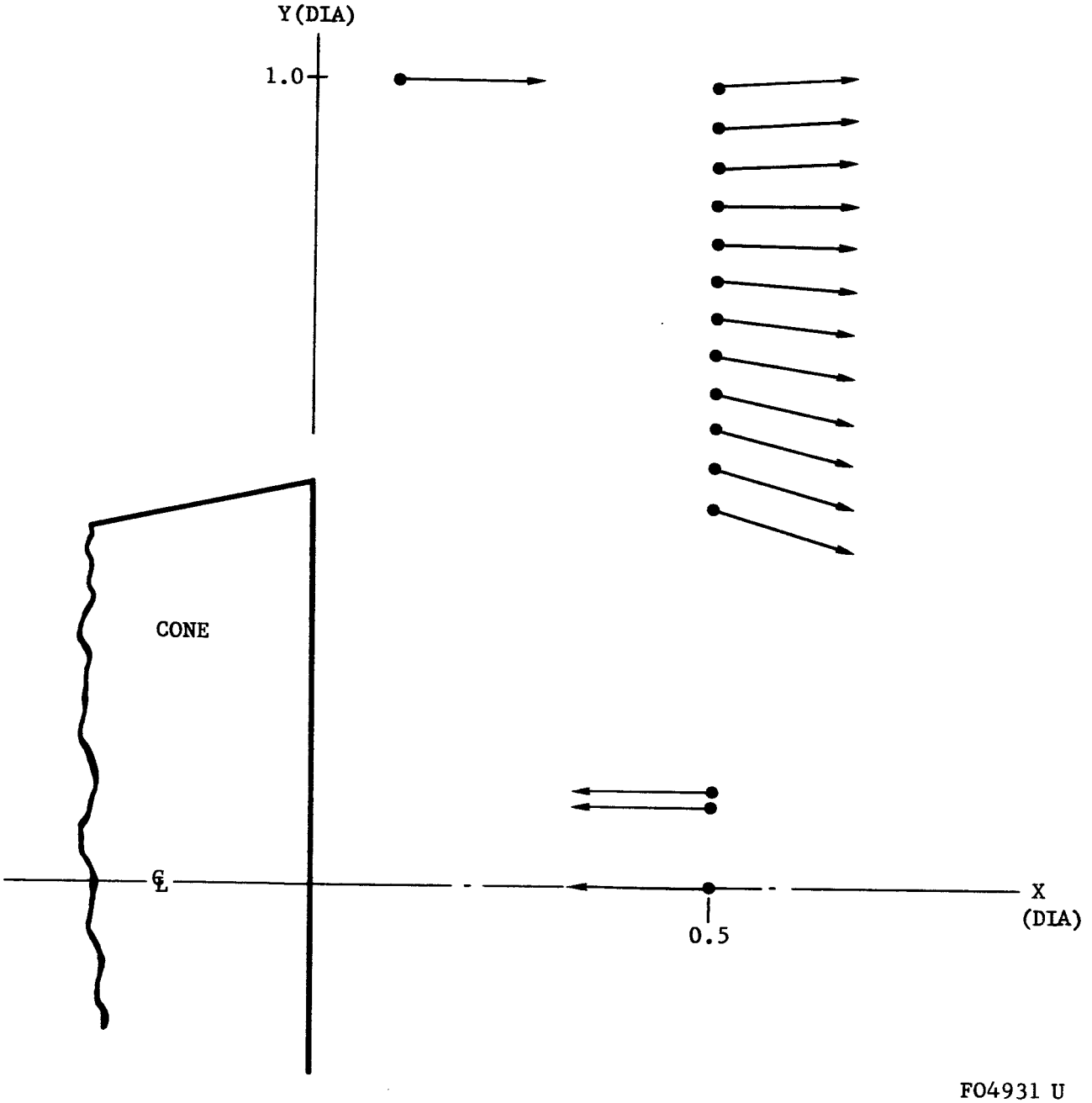

FIGURE 13. MEASURED VELOCITY DIRECTION VECTORS - DOTS SHOW POINT TO WHICH THE MEASUREMENTS REFER

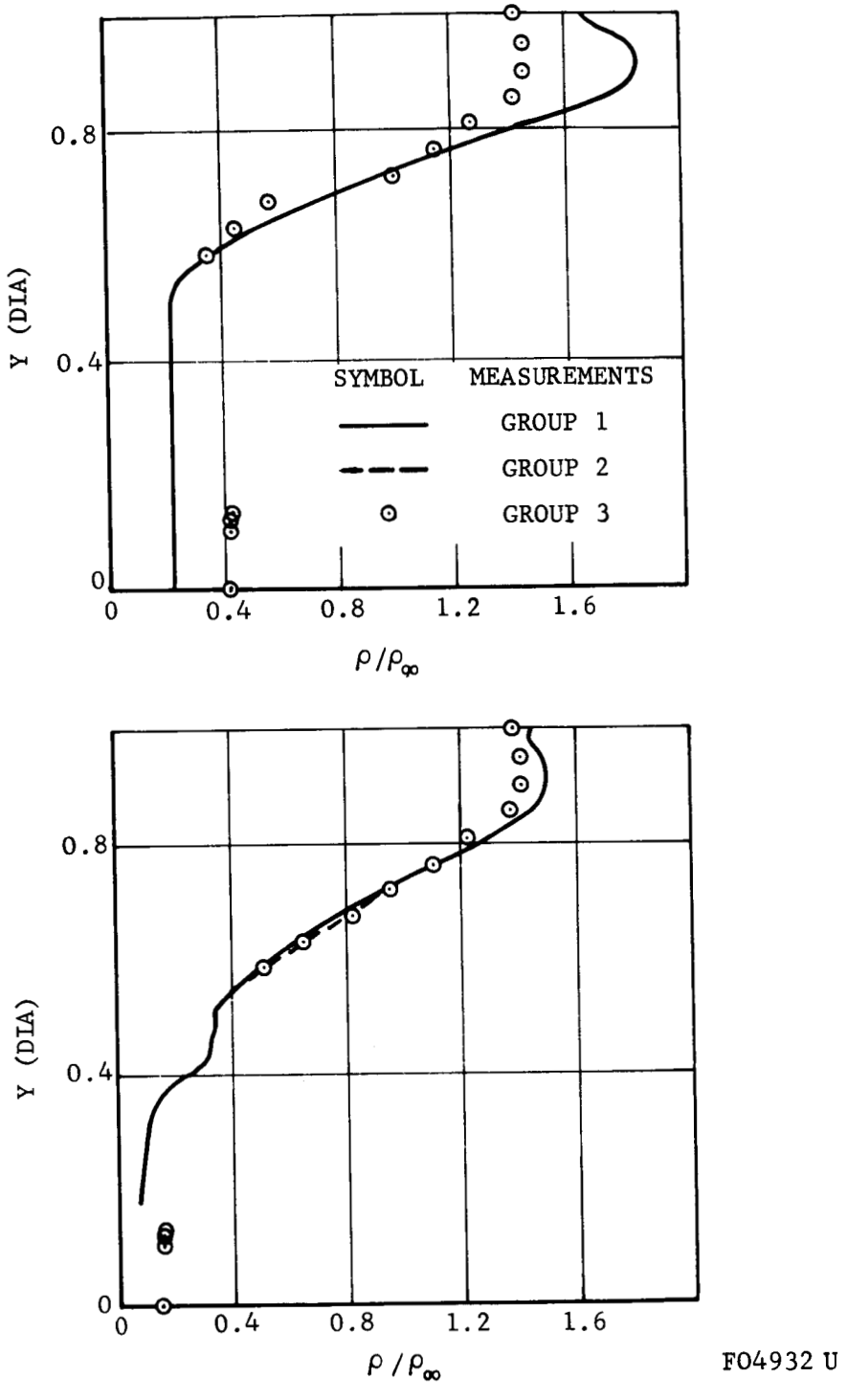

FIGURE 14. STREAM PARAMETERS FOR X = 0.5 DIA BEHIND THE CONE

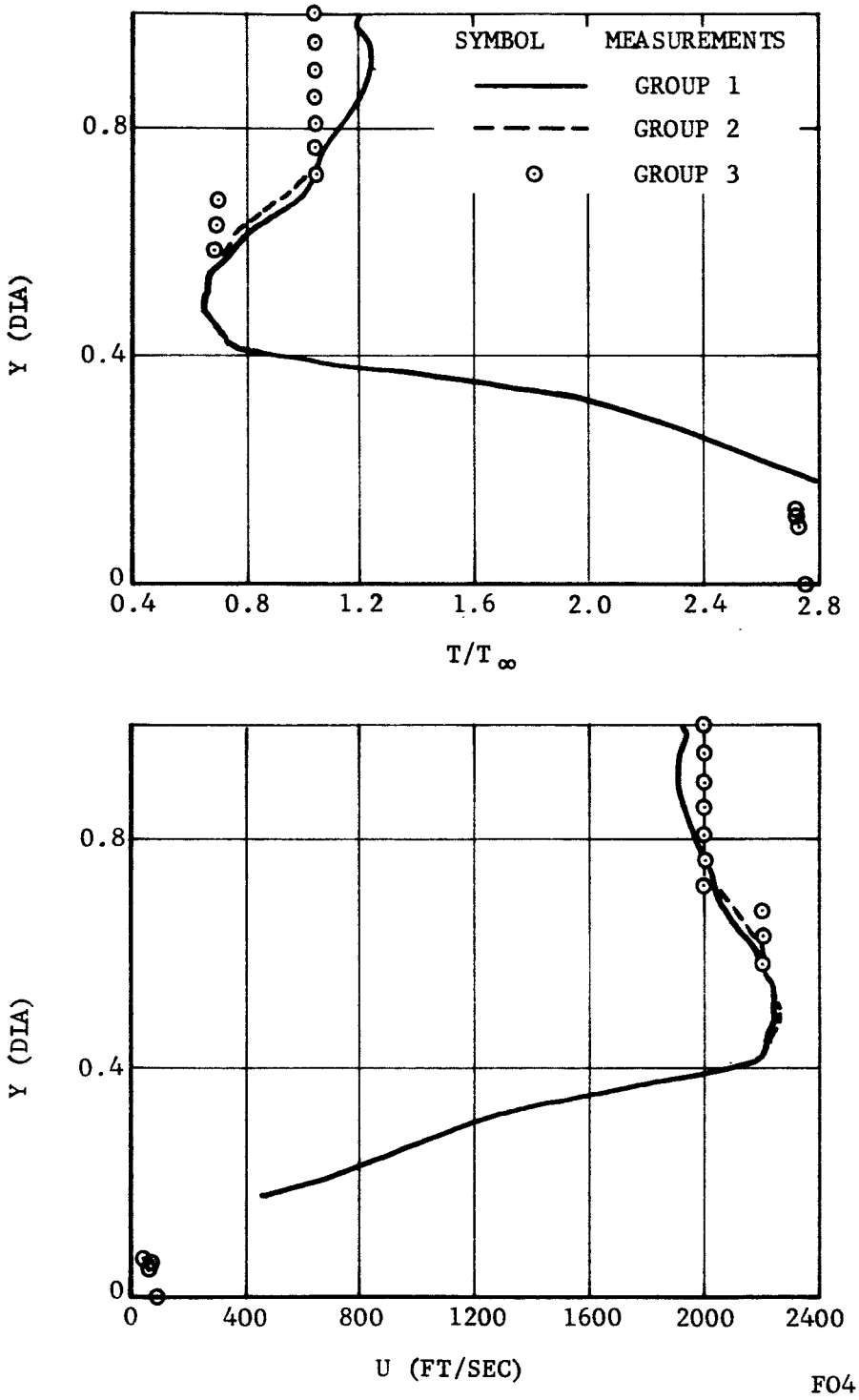

FIGURE 15. STREAM PARAMETERS FOR X = 0.5 DIA BEHIND THE CONE

lines, from Group 2 measurements - p, e_a, i_a, e_b, and i_b; the circular data points, from Group 3 or the two-wire probe measurements - x_o/t_o, e_a, i_a, e_b, and i_b. The measurements were taken at x = 0.5 dia. behind the cone and in the range $0 \leq Y \leq 1.0$ dia. from the cone centerline.

The Group 1 and 2 p, e_a, and i_a measurements were identical, so that the small differences between the two groups is a result of using p_o' in Group 1 as opposed to e_b and i_b in Group 2. The group 2 and 3 e_a, i_a, e_b, and i_b measurements were identical; the differences between the two groups is a result of using p in Group 2 as opposed to x_o/t_o in Group 3.

The greatest problem in obtaining accuracy with the Group 3 data was that of accurately measuring the high speed values of x_o/t_o or U. This is a result of the thermodynamic relation

$$T = T_o - \frac{U^2}{2C_p} \tag{7-1}$$

which was used implicitly in the data reduction process in the form

$$T = \frac{T_o}{1 + \frac{\gamma - 1}{2} M^2} \tag{7-2}$$

and

$$M = \frac{U}{(\gamma \mathcal{R} T)^{\frac{1}{2}}} \tag{7-3}$$

Equations (7-2) and (7-3) may be reduced to (7-1).

If T_o were 300°K and U were 2545 ft/sec, Equation (7-1) gives T = 0. This shows that for T_o near 300°K, as in the present experiments,

an error of only 15% in the measurement of U, whose true value may be 2200 ft/sec, will give values of T which are completely erroneous. Since the Group 3 method of determining p depends on T through the equation of state, $p = \rho RT$, this may also result in erroneous values of p. Therefore, whenever U is so large as to approach the value $(2C_pT_o)^{\frac{1}{2}}$, as may easily be determined in the computer data reduction process, the value of U should be examined for possible errors.

This possibility for error was the reason for limiting the applicability of the two-wire method to $M \leq 3$.[1] A short calculation shows that

$$U \frac{dM}{dU} = M(1 + \frac{\gamma - 1}{2} M^2) \qquad (7\text{-}4)$$

This means that at M = 3, a small percentage error in the measurement of U results in a percentage error 8.4 times as great for $\gamma = 1.4$ in the value of M. However, the ratio is down to 3.6 at M = 2, to 1.2 at M = 1, and to 1.0 at M = 0. Hence, the problem exists only at the larger Mach number.

The Group 1 measurements could not be reduced for $Y < 0.18$ dia. because the p_o' reading was no longer valid. This was partly because of the unknown flow direction in the base recirculation region and partly because of the difficulty of measuring both p and p_o' with accuracy sufficient for meaningful results. The Group 2 measurements were not used near Y = 0 because of difficulty with the data reduction process. An improved computer technique is needed for this region.

No difficulties were experienced in reducing the Group 3 data. The results for T were in reasonable agreement with the Group 1 and 2 results, although the difficulty in measuring U with sufficient accuracy is apparent in the high speed region. In the low speed recirculation region near the axis ($Y < 0.2$), p, ρ, and T were expected to be nearly constant; however, the Group 3 values of p and ρ are significantly larger than the p and ρ of Group 1. This is believed to be a result of the fact that the hot-wire probe was in a reverse flow region. The probe tips used to measure x_o/t_o were designed like those in the lower half of Figure 9 so that the tips apparently did not interfere with the t_o measurement. However, for the e_b and i_b measurements a conventional probe tip was used with the result that the flow must have traveled over the entire probe tip before reaching the hot wire.

Each of the x_o/t_o measurements were repeated several times as a check on the previous results. For the recirculation region of the flow, x_o was 0.028 in. For the high speed regions, x_o was set at 0.240 in. In the shear layer region (near $0.3 < Y < 0.4$), no x_o/t_o measurements were taken, as the stream turbulence made measurement of t_o difficult.

The numbers used in the Group 3 data reduction process are given in Table 1. The wire currents were measured using a digital voltmeter across a precision 10 ohm resistor in series with the hot wire. The digital voltmeter was used to directly measure e_a and e_b; both the voltmeter and a Moseley plotter were used in an automated system for plotting e_a or e_b as a function of Y. The last digit on the voltmeter read in increments of 0.01 mv.

TABLE 1

ℓ = 0.02035 in

d = 0.00010 in

R_L = 1.095 ohms

i_a = 1.000 ma

i_b = 8.494 ma

α = 0.001517/^oK

R_R = 19.354 ohms

Y	x_o/t_o (ft/sec)	e_a (mv)	e_b (mv)
0	52	20.24	239.5
.10	37	20.15	238.4
.12	36	20.13	238.1
.13	23	20.12	238.0
.585	2200	20.68	197.5
.630	2200	20.64	194.0
.674	2200	20.59	190.4
.719	2000	20.53	189.0
.764	2000	20.47	186.5
.809	2000	20.425	184.9
.855	2000	20.385	183.75
.900	2000	20.375	183.45
.950	2000	20.38	183.5
1.000	2000	20.38	183.65

SECTION 8

FLOW REGIME OF PROBE OPERATION

In tests to date the two-wire probe has been operated over a wide range of U, p, ρ, and T. This is illustrated on Figure 16. The upper two points were measured in the subsonic wind tunnel; the four lower points were taken in measuring the cone near wake, as shown on Figures 14 and 15.

8.1 LIMITS OF PROBE OPERATION TO DATE

The probe is useful for measuring flow velocities at Mach numbers much greater than the 3.8 shown on Figure 16, but the corresponding problem of data reduction does not permit the corresponding static pressures and temperatures to be determined accurately unless the Mach number is about 3 or less, as discussed in Section 7.

The probe should also be useful in determining values of p and ρ much larger or smaller than covered by Figure 16, but the present test facilities have not permitted a significantly wider range of test conditions.

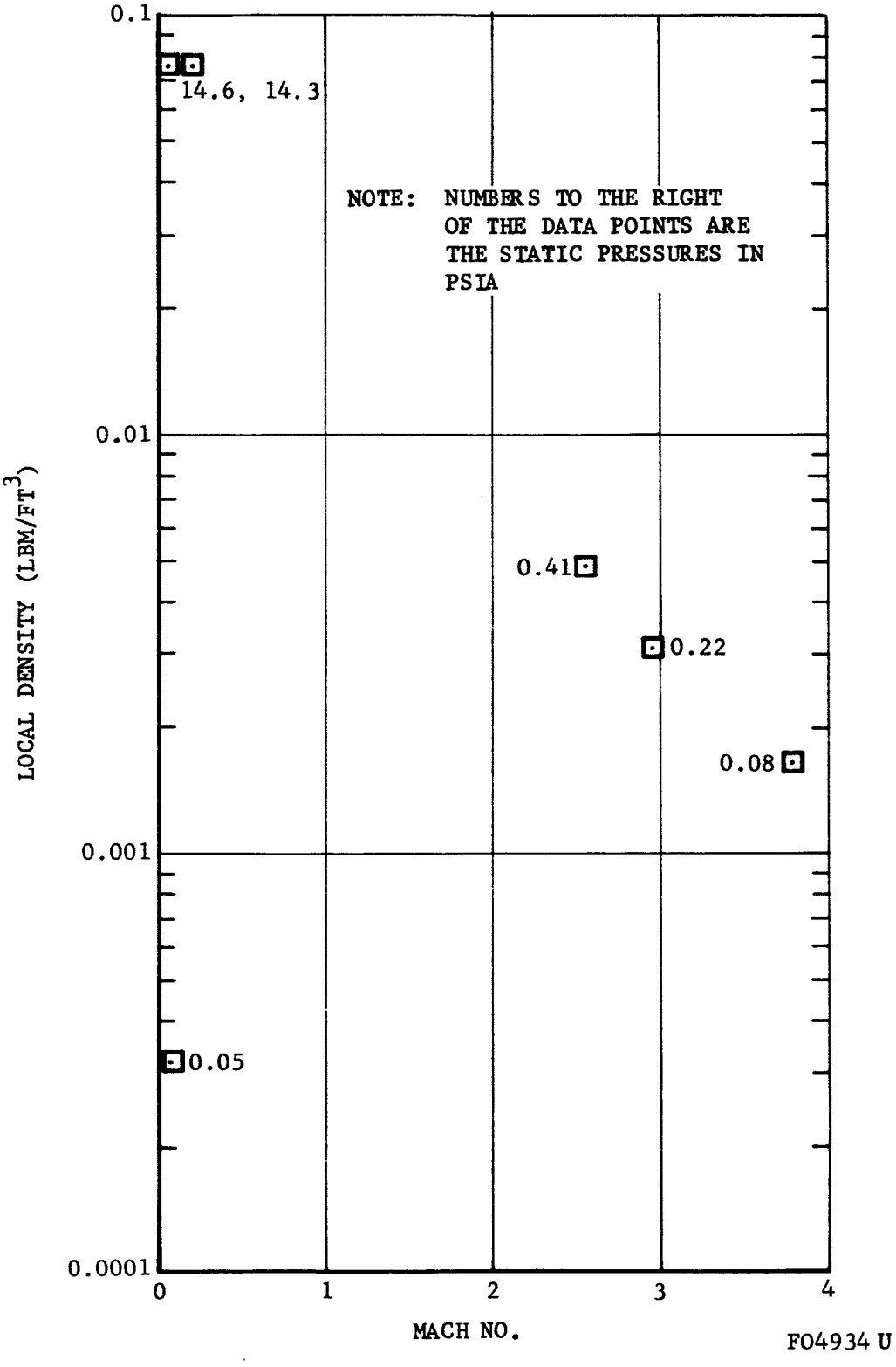

FIGURE 16. FLOW REGIME MAP SHOWING RANGE OF OPERATION OF THE TWO-WIRE PROBE TO DATE

At larger p and ρ, the problem of air loads on the wires becomes greater, and would finally be a limiting factor if p and ρ were increased by too large a factor. For p and ρ greatly reduced from the values of Figure 16, the problem of poor heat transfer to and from the wires would limit the probe operation. In fact, at the lowest point on the figure the Reynolds number R_{xo} based on the length x_o was already so small (about 6) that the heat diffusion of the flow made the determination of the velocity vector direction difficult. The correspondingly small Nusselt number of the second wire made the t_o measurement difficult.

8.2 IMPROVEMENT IN PROBE OPERATING LIMITS THROUGH FUTURE RESEARCH

Two areas of future research should be helpful in setting limitations to the probe operation. The first is an improved wire material, as discussed in Section 3 for application to wire 1. If this material (92% Pt, 8% W) can be mounted in the probe tips without difficulty, as may be expected, its greater strength and resistivity should make possible the transmission of a much larger heat pulse to the second wire.

The larger heat pulse would be a very welcome improvement. The signals received by the second wire to date often have been partially masked by apparent flow turbulence; thus, the larger heat pulse should clarify the heat signal.

This leads to the second area for research. Because of the problem of turbulent masking of the signal, an analysis should be performed to see what levels of turbulence will provide a turbulent signal capable

of masking the heat signal. The analysis should be checked by placing the two-wire probe in an experimental facility where the turbulence level can be varied over a wide range and independently measured for its amplitude. Then, the maximum turbulence amplitude for which the turbulence does not greatly interfere with probe measurements can be mapped as a function of the mean flow variables.

SECTION 9

CONCLUSIONS

A probe has been developed which carries two hot-wire elements. This has led to the following conclusions:

1. The probe may be used to manipulate the wires in a gas stream so that a heat pulse generated by the first wire may be sensed by the second wire to determine the flow direction.

2. The probe may be used to measure flow speeds from almost 0 to over 2000 feet/sec provided that the flow static pressure and density do not exceed certain rather wide limits.

3. The data taken from the hot-wire elements can be used to compute the stream variables - pressure, density, temperature, and Mach number - provided that the Mach number is not greater than about 3. The probe may be used at low subsonic speeds as well as at supersonic speeds.

4. A machine program is required for rapid computation of the flow variables.

5. The probe is useful only in regions where the flow turbulence does not exceed a certain amount.

SECTION 10

REFERENCES

1. "Instrument Development for the Base Flow Region of a Multi-Nozzle Booster Vehicle," Aeronutronic Publication No. P-24105 (U), Dec. 9, 1964.
2. Bauer, A. B., "Direct Measurement of Velocity by Hot-Wire Anemometry," AIAA Journal 3, pp. 1189-1191.
3. "Instrument Development for the Base Flow Region of a Multi-Nozzle Booster Vehicle," Bi-Monthly Progress Report No. 1, Aeronutronic Publication No. U-3253, Sept. 1, 1965.
4. "Instrument Development for the Base Flow Region of a Multi-Nozzle Booster Vehicle," Bi-Monthly Progress Report No. 2, Aeronutronic Publication No. U-3334, Nov. 1, 1965.
5. "Instrument Development for the Base Flow Region of a Multi-Nozzle Booster Vehicle," Bi-Monthly Progress Repot No. 3, Aeronutronic Publication No. U-3397, Dec. 30, 1965.

6. Schlichting, H., "Boundary Layer Theory," Chapt. IX, Mc-Graw-Hill, 1955.

7. Stalder, J. R., Goodwin, G., and Creager, M. O., "A Comparison of Theory and Experiment for High-Speed Free-Molecule Flow," NACA Report 1032, 1951.

8. Emmons, H. W., "Fundamentals of Gas Dynamics," High Speed Aerodynamics and Jet Propulsion Vol. III, Princeton University Press, 1958.

9. Dewey, C. F., Jr., "Hot-Wire Measurements in Low Reynolds Number Hypersonic Flows," ARS Journal 31, pp. 1709.

10. Pritts, O. R., Lockheed Missiles and Space Company, Huntsville, Ala., private communication, May, 1966.

11. "Instrument Development for the Base Flow Region of a Multi-Nozzle Booster Vehicle," Bi-Monthly Progress Report No. 4, Aeronutronic Publication No. U-3484, Feb. 28, 1966.

12. Dewey, C. F., Jr., "Hot-Wire Measurements in Low Reynolds Number Hypersonic Flows," GALCIT Hypersonic Research Project, Mem. No. 63, Sept. 15, 1961.

13. Dewey, C. F., Jr., "A Correlation of Convective Heat Transfer and Recovery Temperature Data for Cylinders in Compressible Flow," Int. J. Heat Mass Transfer 8, pp. 245-252, Pergamon Press, 1965.

14. Demetriades, A., and Bauer, A. B., "Supersonic Wind Tunnel Experiments with Axisymmetric Wakes," AIAA Paper No. 66-453, to be presented at Los Angeles, June 27-29, 1966.